

X-ray and Phase Space Density Constraints on the Properties of the Dark Matter Particle

Casey R. Watson
Millikin University

July 23, 2014

Many Thanks to

My Collaborators:

Peter Biermann (MPI, Univ. of Bonn, Univ of AL), Zhiyuan
Li (CfA/UCLA) & Joe Cheeney, Chris Pelikan, Nick Polley,
Leon Yu (Millikin)
and

Norma and Hector for inviting me.

OUTLINE

- **Properties of Sterile Neutrinos**
- **Models of Sterile Neutrino Interactions & Production**
- **X-ray Constraints from Previous Studies**
 - CXB
 - Galaxy Clusters
 - Dwarf Galaxies
- **The Advantages of Andromeda**
- **Constraints from *XMM* Observations of Andromeda**
- **Constraints from *Chandra* Observations of Andromeda**
- **The Bulbul et al. (2014) Anomaly in Context**
 - vs. X-ray Constraints
 - vs. Galaxy Constraints
- **Improved Phase Space Density Constraints via MW dSphs**
 - Implications for DM Particle mass + Galaxy Formation/Evolution

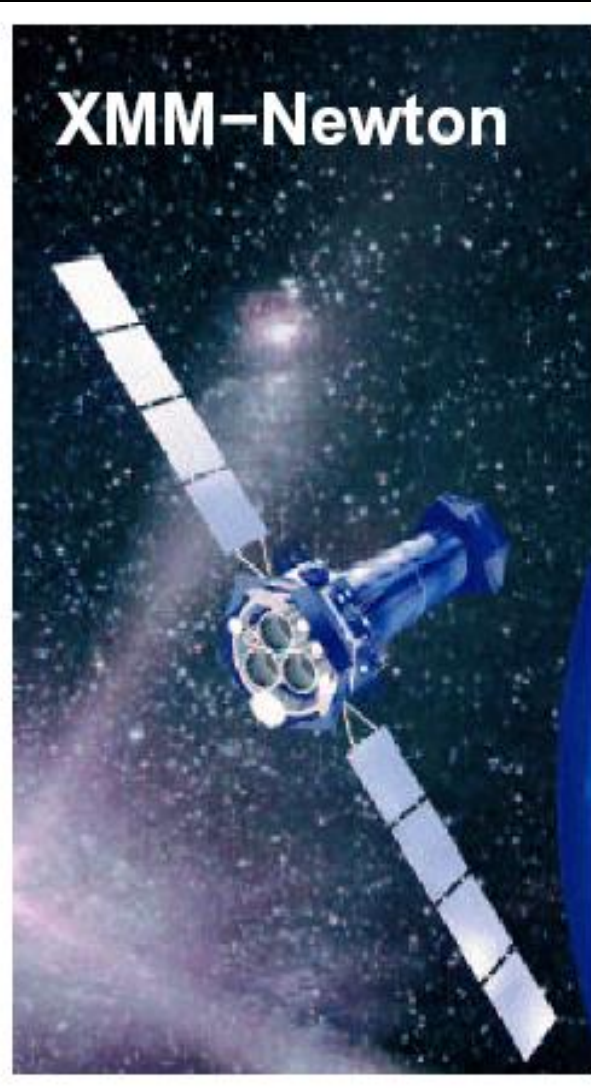
The Fertile Phenomenology of Sterile Neutrinos

- Non-zero active neutrino masses [1,2]
- Baryon & Lepton Asymmetries [15-20]
- Big Bang Nucleosynthesis [19]
- Evolution of the matter power spectrum [21,22]
- Reionization [23-31]
- Active Neutrino Oscillations [32-33]
- Pulsar Kicks [34-39]
- Supernovae [40-42]
- Excellent Dark Matter Particle Candidate [3-14, 43-57]
- *Most Importantly: Readily Testable*
 - *Can decay into detectable X-ray photons*

Detecting Sterile Neutrino Radiative Decays:

$$“\nu_s” \rightarrow “\nu_\alpha” + \gamma$$

$$E_\gamma = \frac{m_s}{2} \sim 1 \text{ keV}$$



If

$1 \text{ keV} < m_s < 20 \text{ keV}$,

Chandra & XMM

can detect the

X-ray photons

associated with

sterile neutrino

radiative decays.

Sterile Neutrino Interactions with SM Particles

(Abazajian, Fuller, Patel 2001 [5]; Abazajian, Fuller, Tucker 2001 [6])

Very small mixing ($\sin^2 2\theta \lesssim 10^{-7}$) *between*

mass $|\nu_{1,2}\rangle$ &

flavor $|\nu_{\alpha,s}\rangle$ states:

$$\begin{aligned} |\nu_\alpha\rangle &= \cos\theta |\nu_1\rangle + \sin\theta |\nu_2\rangle \\ |\nu_s\rangle &= -\sin\theta |\nu_1\rangle + \cos\theta |\nu_2\rangle \end{aligned}$$

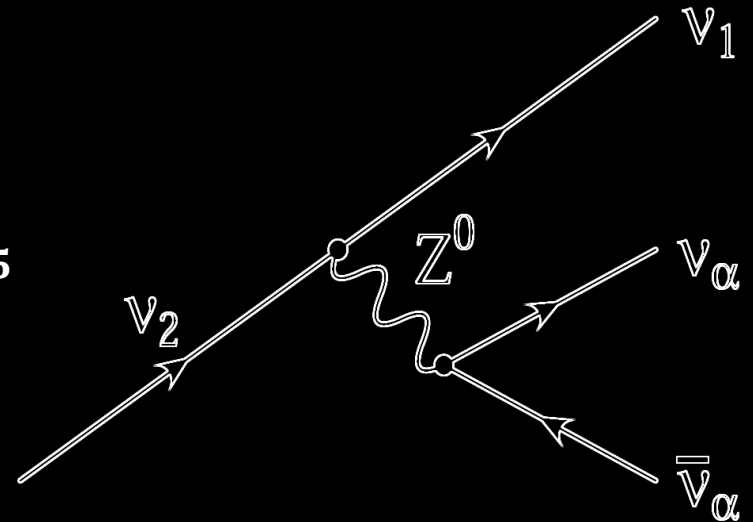
For $m_s < m_e$,

3 ν Decay Mode Dominates:

$$\Gamma_{3\nu} \simeq 1.74 \times 10^{-30} s^{-1} \left(\frac{\sin^2 2\theta}{10^{-10}} \right) \left(\frac{m_s}{\text{keV}} \right)^5$$

Radiative Decay Rate is:

$$\Gamma_s \simeq 1.36 \times 10^{-32} s^{-1} \left(\frac{\sin^2 2\theta}{10^{-10}} \right) \left(\frac{m_s}{\text{keV}} \right)^5$$



$$\nu_s \rightarrow \nu_\alpha + \gamma$$

The Sterile Neutrino Radiative Decay Signal:

- Radiative Decay Luminosity:

$$\begin{aligned} L_{x,s} &= E_{\gamma,s} N_s^{FOV} \Gamma_s = \frac{m_s}{2} \left(\frac{M_{DM}^{FOV}}{m_s} \right) \Gamma_s \\ &\simeq 1.2 \times 10^{33} \text{ erg s}^{-1} \left(\frac{M_{DM}^{FOV}}{10^{11} M_{\odot}} \right) * \left(\frac{\sin^2 2\theta}{10^{-10}} \right) \left(\frac{m_s}{\text{keV}} \right)^5 \end{aligned}$$

- Measured Flux: $\Phi_{x,s} = \frac{L_{x,s}}{4\pi D^2}$

$$\begin{aligned} \Phi_{x,s}(\sin^2 2\theta) &\simeq 1 \times 10^{-17} \text{ erg cm}^{-2} \text{ s}^{-1} \left(\frac{D}{\text{Mpc}} \right)^{-2} \\ &\times \left(\frac{M_{DM}^{FOV}}{10^{11} M_{\odot}} \right) \left(\frac{\sin^2 2\theta}{10^{-10}} \right) \left(\frac{m_s}{\text{keV}} \right)^5 \end{aligned}$$

Sterile Neutrino Production:

- Dodelson-Widrow Model [3]

- Density-Production Relationship [43]:

$$m_s = 55.5 \text{ keV} \left(\frac{\sin^2 2\theta}{10^{-10}} \right)^{-0.615} \left(\frac{\Omega_s}{0.24} \right)^{0.5}$$

(for $T_{\text{QCD}} \sim 170 \text{ MeV}$)

- Mixing Angle-Independent Flux:

$$\begin{aligned} \phi_{x,s}(\Omega_s) \simeq & 7.0 \times 10^{-15} \text{ erg cm}^{-2} \text{ s}^{-1} \left(\frac{D}{\text{Mpc}} \right)^{-2} \\ & \times \left(\frac{M_{DM}^{FOV}}{10^{11} M_{\odot}} \right) \left(\frac{\Omega_s}{0.24} \right)^{0.813} \left(\frac{m_s}{\text{keV}} \right)^{3.374} \end{aligned}$$

- Agrees with Asaka et al. model [48] for

$$1 \text{ keV} \lesssim m_s \lesssim 10 \text{ keV}$$

To maximize the sterile neutrino decay signal:

$$\Phi_{x,s}(\sin^2 2\theta) \simeq 1.0 \times 10^{-17} \text{ erg cm}^{-2} \text{ s}^{-1} \left(\frac{D}{\text{Mpc}} \right)^{-2} \\ \times \left(\frac{M_{DM}^{FOV}}{10^{11} M_{\odot}} \right) \left(\frac{\sin^2 2\theta}{10^{-10}} \right) \left(\frac{m_s}{\text{keV}} \right)^5$$

the ideal object to study is:

- nearby: small Distance D ,
- massive: large M_{DM} (in FOV),
- quiescent: low astrophysical background.

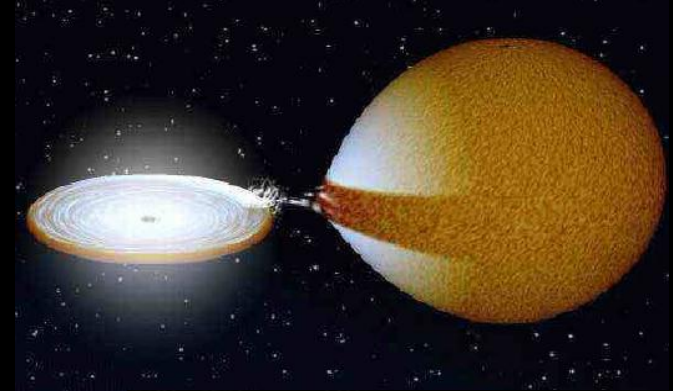
Astrophysical X-ray Sources:

Stellar Sources:

HMXB: Fueled by stellar wind;
widely-separated



LMXB: Roche Lobe accretion;
Contact Binary systems

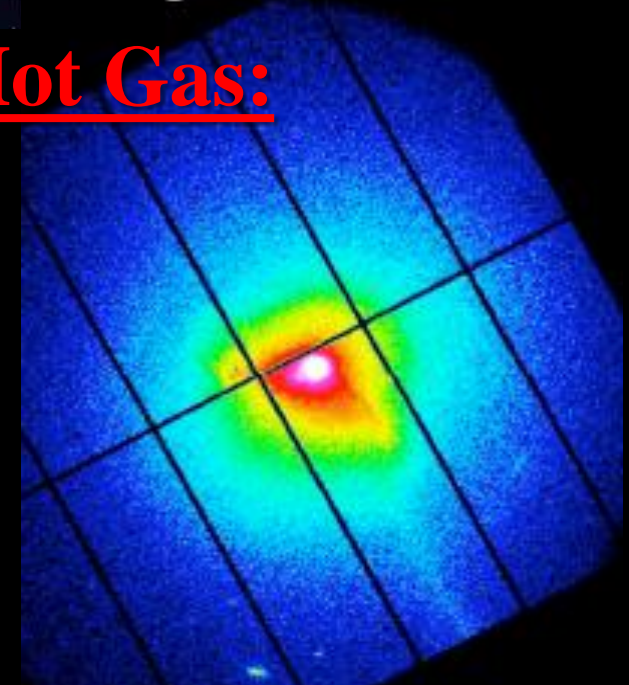


The Virgo Cluster

AGN: Fueled by accretion onto
Supermassive BHs



Hot Gas:



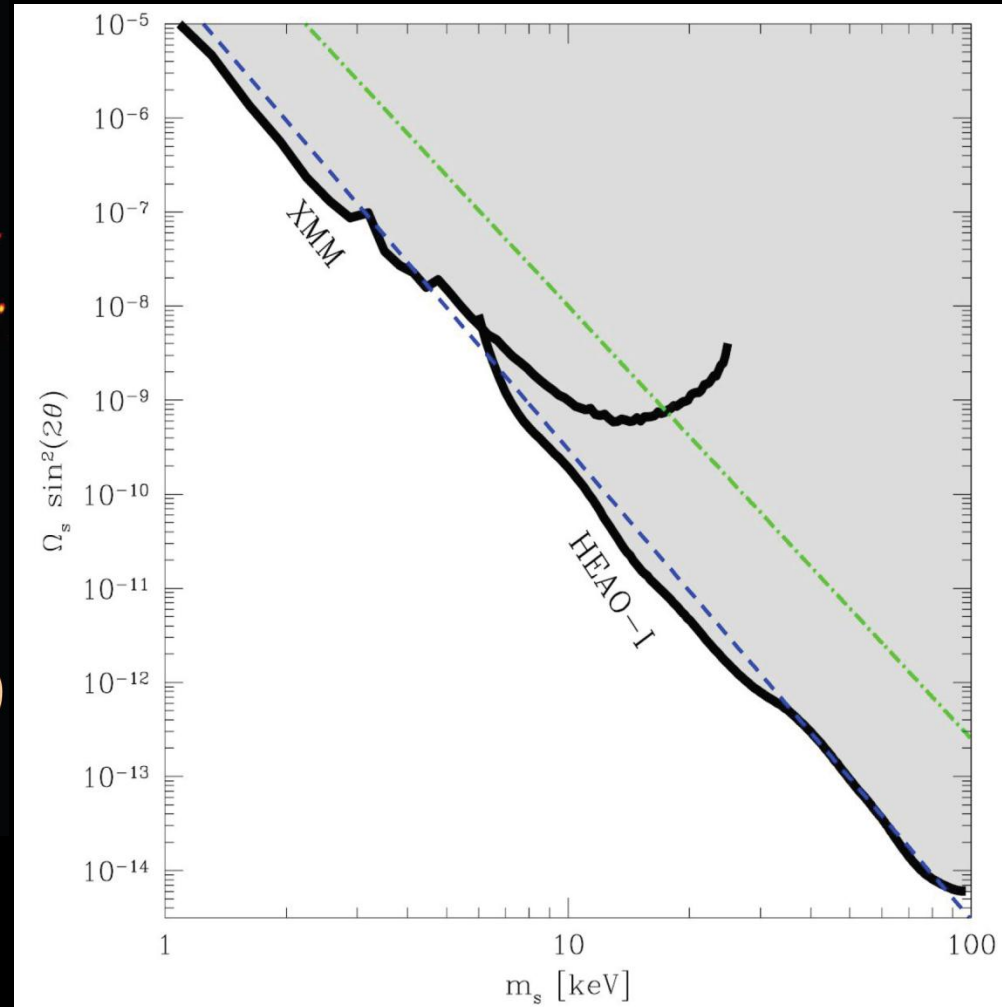
Nuclear & Diffuse Sources:

Previous work I: Cosmic X-ray Background

Cosmic X-ray
Background

HUGE range of $m_s - \sin^2 2\theta$
probed via combined
XMM & HEAO-I Data [61].

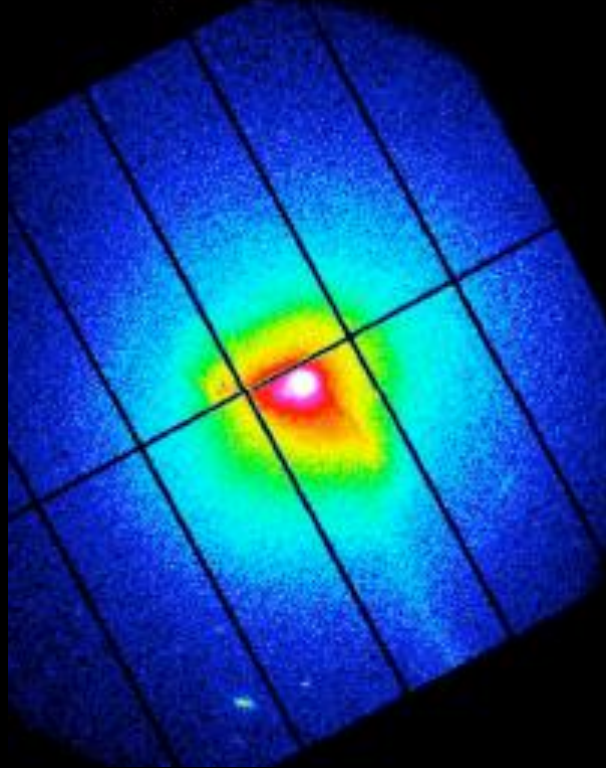
Rekindled interest in m_s
X-ray constraints [6].



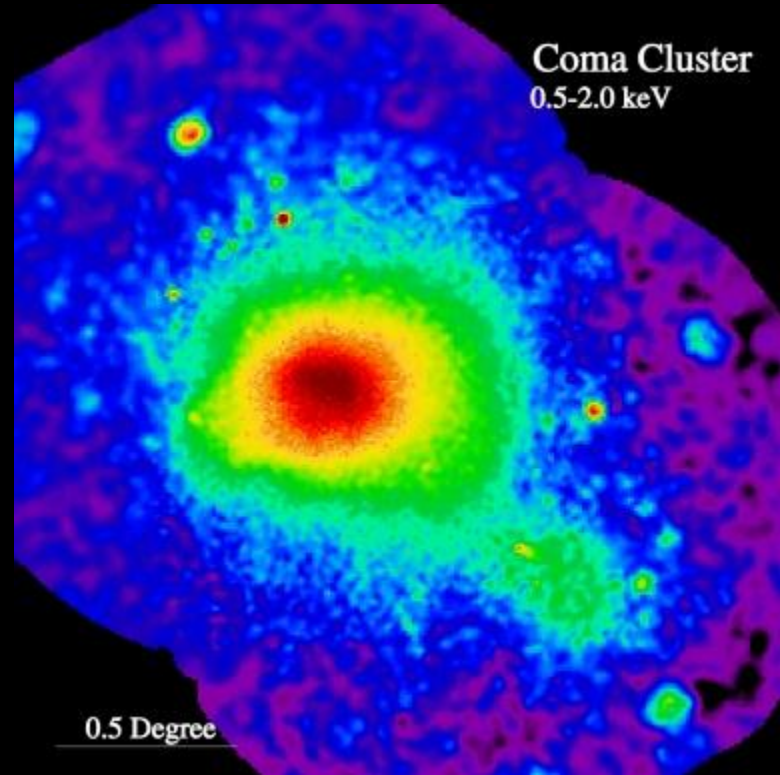
Constraints: $m_s < 9.3$ keV
(for DW Model ν_s [3, 43]).

Previous work II: Galaxy Clusters

The Virgo Cluster



Coma Cluster
0.5-2.0 keV



Advantage: HUGE $M_{DM} \sim 10^{13} M_{\odot}$

PROBLEMS: HUGE background; $D > 10$ Mpc

Constraints (for DW Model ν_s [3, 43]):

$m_s < 8.2$ keV (Virgo [44]); $m_s < 6.3$ keV (Virgo + Coma [13, 63]).

Advantages of Andromeda (M31)

(Watson, Li, Polley 2012, Watson, Beacom, Yuksel, Walker 2006 [66])

Nearby: $D = 0.78 \pm 0.02$ Mpc [102, 103]

LOW astrophysical background (little hot gas & bright point sources can be excised)

Well-measured Dark Matter Distribution

based on analyses of extensive Rotation Curve Data

(Klypin, Zhao, Somerville 2002 [104], Seigar, Barth, & Bullock 2007 [105])

Prospective Sterile Neutrino Signals

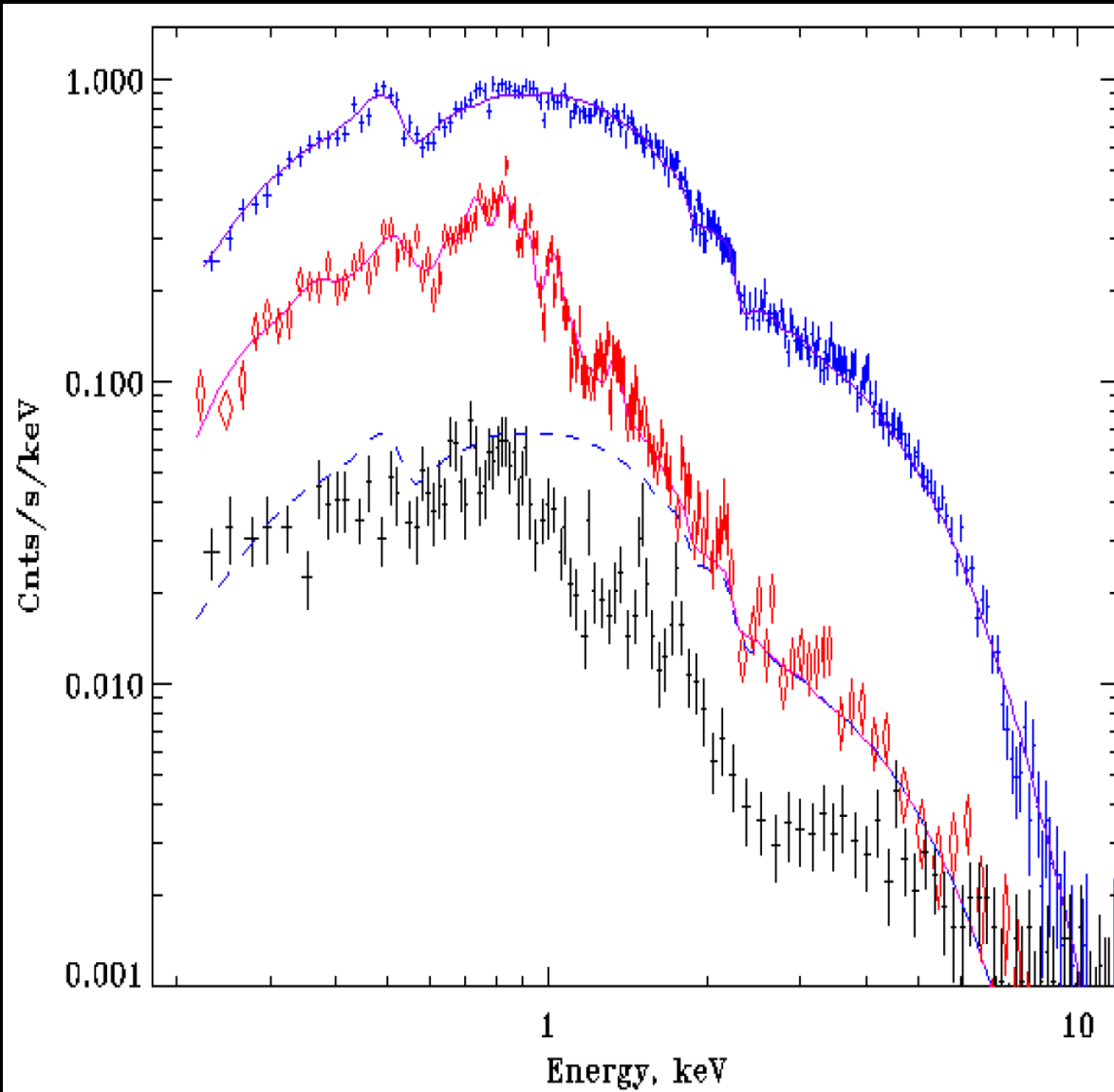
Comparable to Massive Clusters without the background

Exceeding Ultra Nearby Dwarf Galaxies

$$\frac{\Phi_{\text{M31}}}{\Phi_{\text{Clus}}} = \left(\frac{M_{\text{M31}}^{\text{FOV}}}{M_{\text{Clus}}^{\text{FOV}}} \right) \left(\frac{D_{\text{Clus}}}{D_{\text{M31}}} \right)^2 \simeq \frac{\Phi_{\text{M31}}}{\Phi_{\text{Dwarf}}} = \left(\frac{M_{\text{M31}}^{\text{FOV}}}{M_{\text{Dwarf}}^{\text{FOV}}} \right) \left(\frac{D_{\text{Dwarf}}}{D_{\text{M31}}} \right)^2 \gtrsim 1$$

Unresolved 5' XMM Spectrum of Andromeda

(from Shirey et al. 2001 [96])



REDUCED

Astrophysical

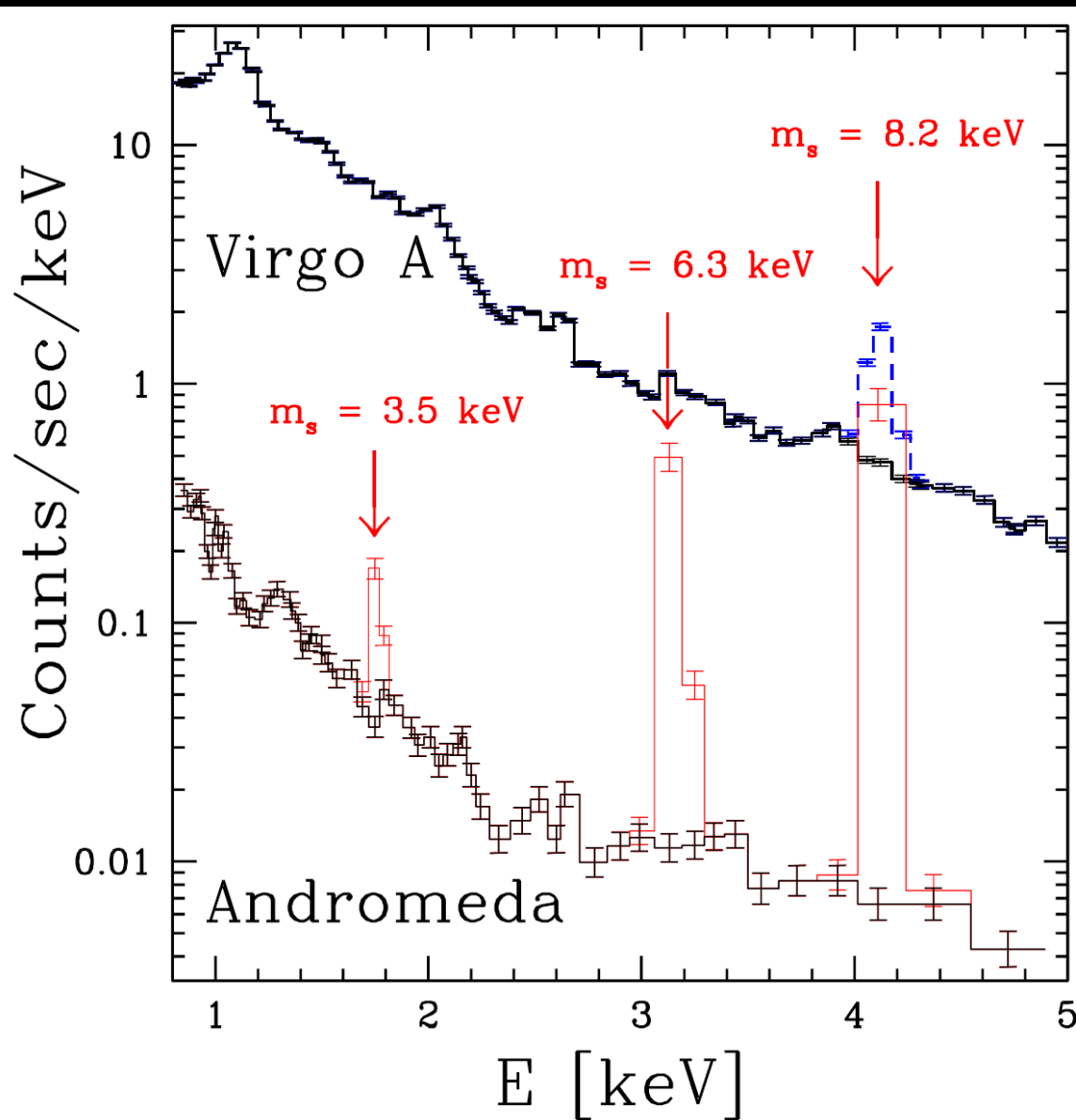
Background:

Bright point sources
removed (in Ref. [96])

Intrinsically LOW
hot gas emission

RESULTS

For $\Omega_s = 0.24$ & $L = 0$ density-production relationship [43]:



Andromeda:

$m_s < 3.5$ keV

[66]

Virgo A:

$m_s < 8.2$ keV

[44]

Virgo A+Coma:

$m_s < 6.3$ keV

[13, 63]

$m_s = 6.3$ keV & $m_s = 8.2$ keV
decay peaks are also shown
relative to Andromeda data.

Previous work III: Dwarf Galaxies

LMC

MAX ACIS-I FoV



Ursa
Minor

$$R_{\text{FoV}} \simeq 0.3 \text{ kpc} \left(\frac{\theta}{1'} \right) \left(\frac{r}{\text{Mpc}} \right)$$

$$\text{so } R_{\text{Max FoV}}^{\text{LMC}} \simeq 0.3 \text{ kpc} \left(\frac{17'}{1'} \right) \left(\frac{45 \text{ kpc}}{\text{Mpc}} \right) \simeq 0.23 \text{ kpc!!}$$

Advantages: Small D; Low background

PROBLEMS: Low & Uncertain M_{DM} in FOV.

Constraints (for DW Model v_s [3, 43]):

$$m_s < 3 \text{ keV}^{**} \text{ (LMC + MW) [69]}$$

**** VERY WEAK EXCLUSION CRITERION**

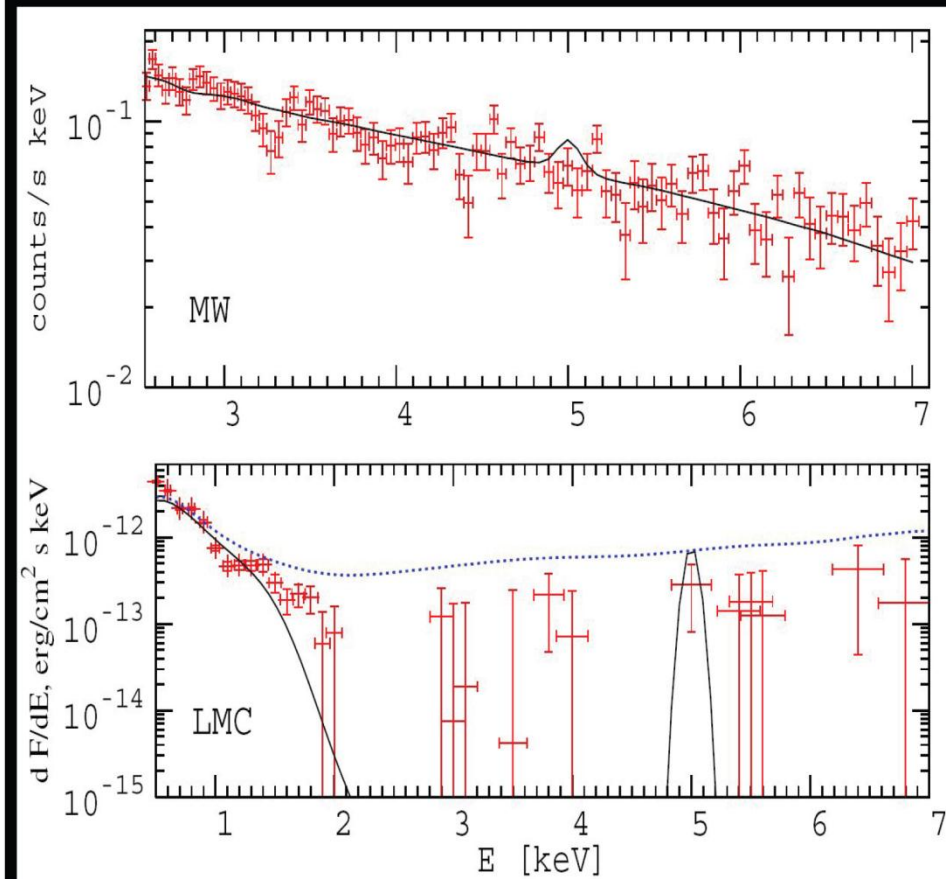
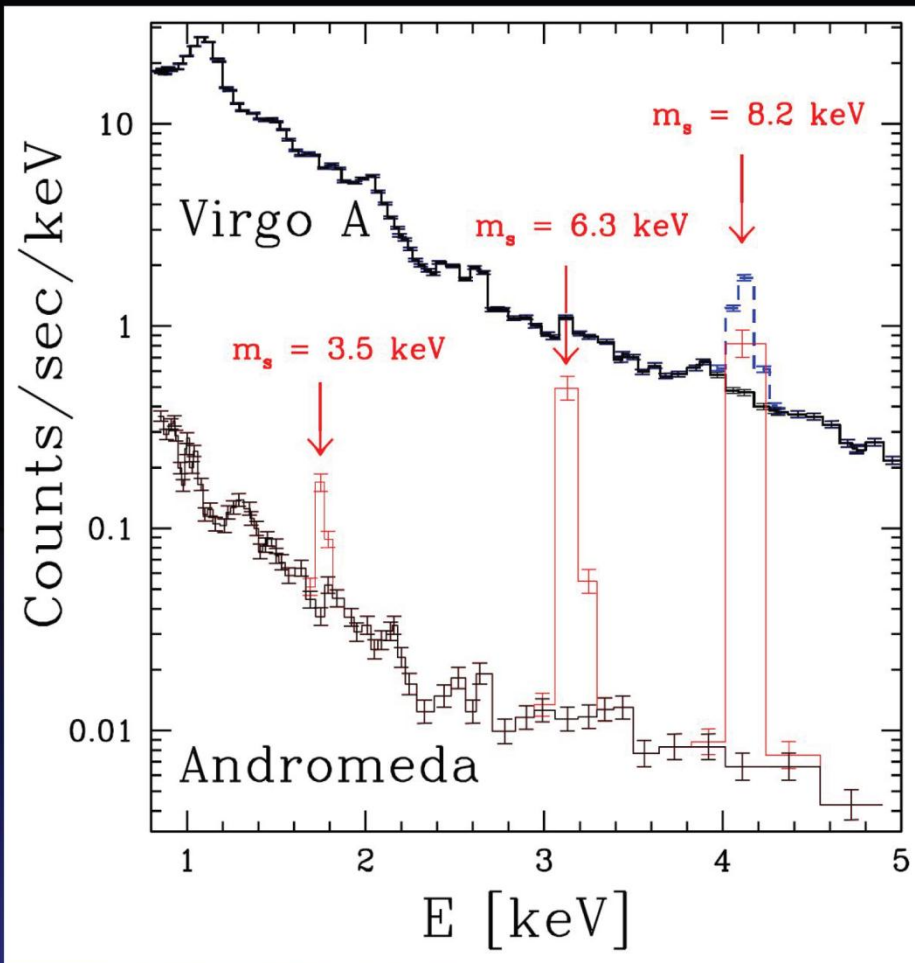
Andromeda (XMM) vs. Dwarf/MW Constraints

Andromeda [66] &

LMC + MW [69]

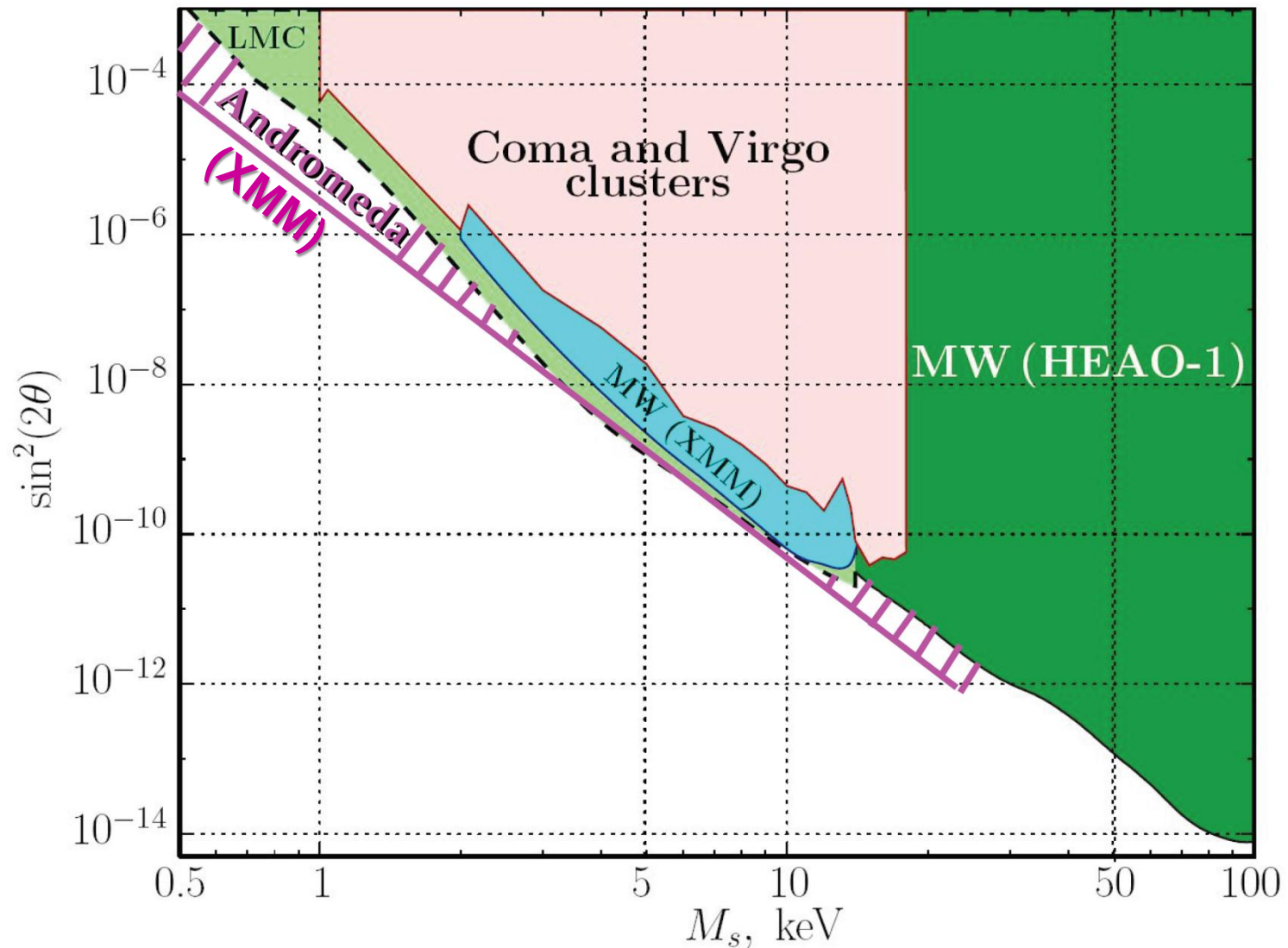
(Watson, Beacom, Yüksel, Walker 2006)

(Boyarsky, Neronov, Ruchayskiy, Shaposhnikov, Tkachev 2006)



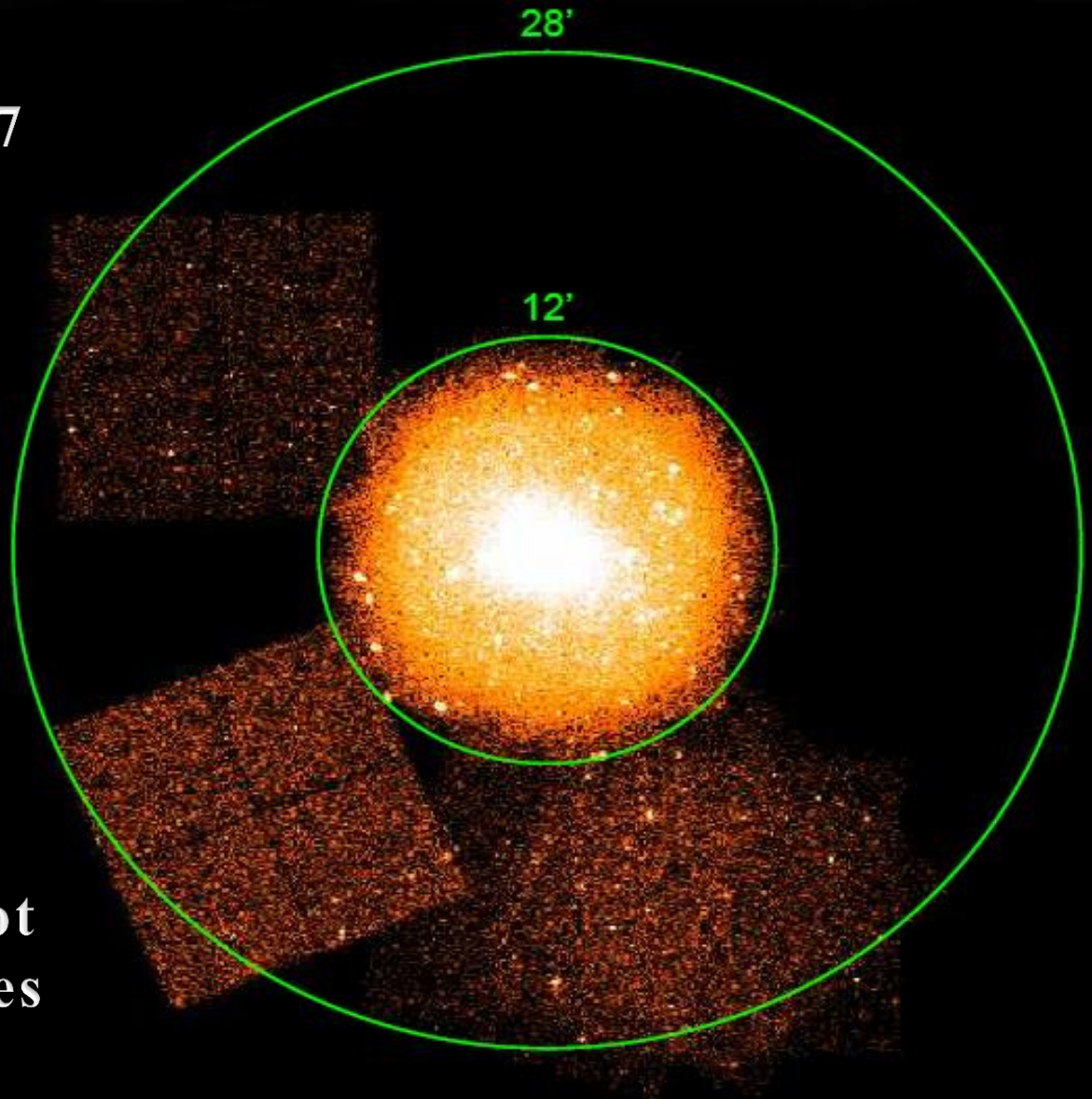
Andromeda (XMM) vs. Cluster/Dwarf/MW

Andromeda (Watson, Beacom, Yüksel, Walker 2006) vs.
LMC + **MW** (Boyarsky, Neronov, Ruchayskiy, Shaposhnikov, Tkachev 2006)



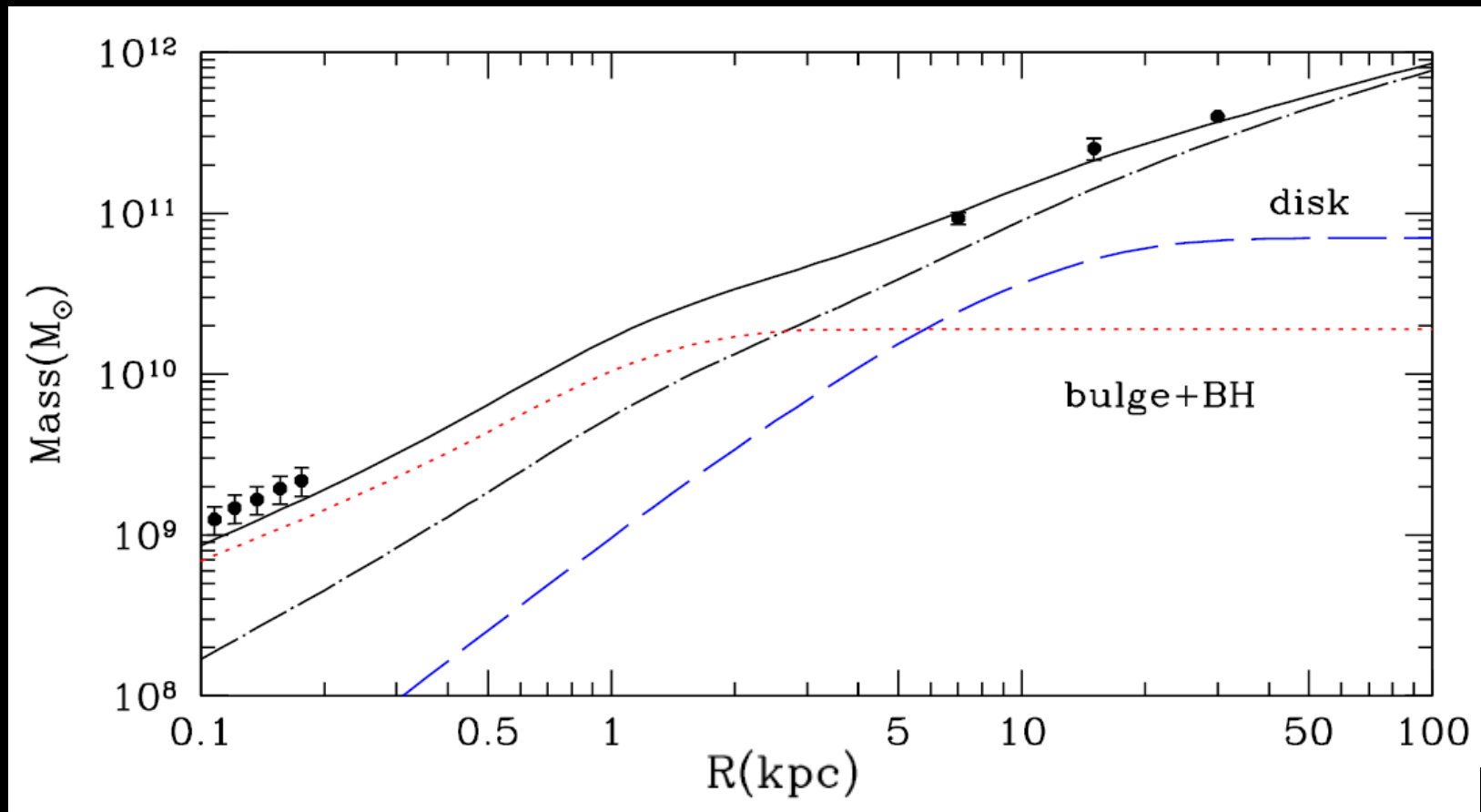
Chandra FOV of M31: $\Delta\theta = 12' - 28'$

- Raw counts associated with the 7 Chandra ACIS-I exposure regions.
- Exposure times range from 5ks to 20ks
- Central $12'$ is excluded because of high astrophysical background from hot gas and point sources in that region



Andromeda's

Well-measured Matter Distribution:

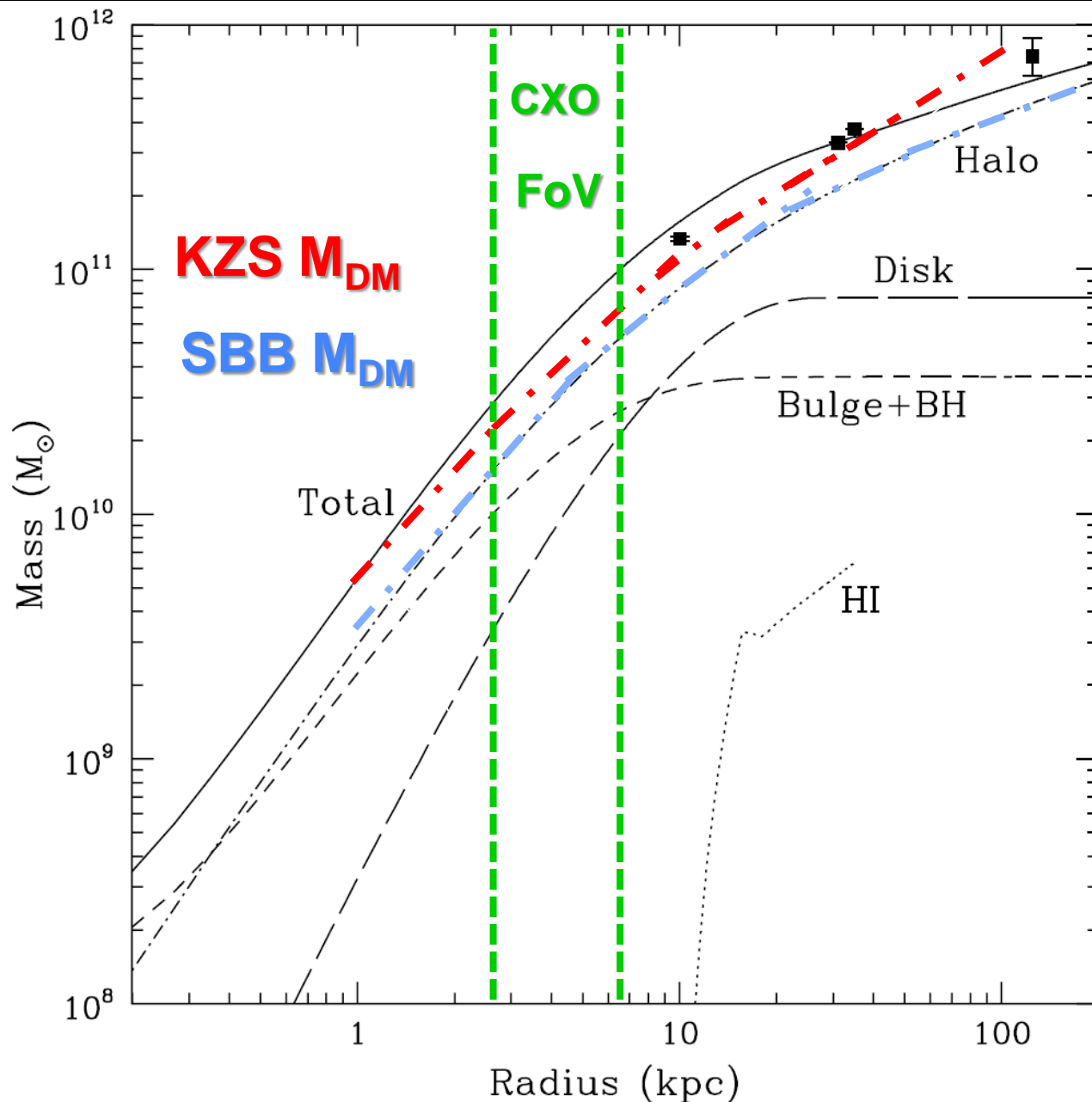


Constraints at small radii are from Stellar Motions in the Nucleus.
Three points at $R > 5$ kpc characterize the spread in $v_{\text{rot}} = 255 \pm 15$ km/s.

(Klypin, Zhao, Somerville 2002 [104] (KZS))

(Additional Data & updated analysis in Seigar, Barth, & Bullock 2007 [105] (SBB))

More Conservative DM Matter Distribution:



SBB M_{DM}

<

KZS M_{DM}

by a factor of

$\sim 1.05 - 1.2$

in *Chandra* FoV

SBB M_{DM}

<

Burkert M_{DM}
[67, 106]

by a factor of

$\sim 1.2 - 1.4$

in *Chandra* FoV

The Fraction of **Andromeda's** Dark Matter Mass in the *Chandra* field of view (FOV):

$$\rho_{\text{DM}}(|\vec{r} - \vec{D}|)$$

(from Seigar, Barth, & Bullock 2007
[105])

$$d\Sigma_{\text{FOV}} = \frac{\rho_{\text{DM}}(|\vec{r} - \vec{D}|) dV_{\text{fov}}}{r^2}$$

\vec{r}

\vec{D}

$|\vec{r} - \vec{D}|$

$\Delta\theta_{\text{FOV}} = 12' - 28'$

Andromeda
Halo

$$M_{\text{DM}}^{\text{FOV}} = D^2 \Sigma_{\text{DM}}^{\text{FOV}}$$

$$\Sigma_{\text{DM}, \text{M31}}^{\text{FOV}} \simeq (0.8 \pm 0.04) \times 10^{11} M_{\odot} \text{Mpc}^{-2}$$

$$M_{\text{DM}, \text{M31}}^{\text{FOV}} \simeq (0.49 \pm 0.05) \times 10^{11} M_{\odot}$$

Conversion of Decay Signal to Detector Units:

$$\begin{aligned} \frac{dN_{\gamma,s}}{dE_{\gamma,s}dt}(\Omega_s) &= \left(\frac{\Phi_{x,s}(\Omega_s)}{E_{\gamma,s}} \right) \left(\frac{A_{\text{eff}}(E_{\gamma,s})}{\Delta E} \right) \\ &= 6.7 \times 10^{-2} \text{ Counts/sec/keV} \left(\frac{A_{\text{eff}}(E_{\gamma,s})}{100 \text{ cm}^2} \right) \\ &\times \left(\frac{\Sigma_{\text{DM}}^{\text{FOV}}}{10^{11} M_{\odot} \text{Mpc}^{-2}} \right) \left(\frac{\Omega_s}{0.24} \right)^{0.813} \left(\frac{m_s}{\text{keV}} \right)^{1.374} \end{aligned}$$

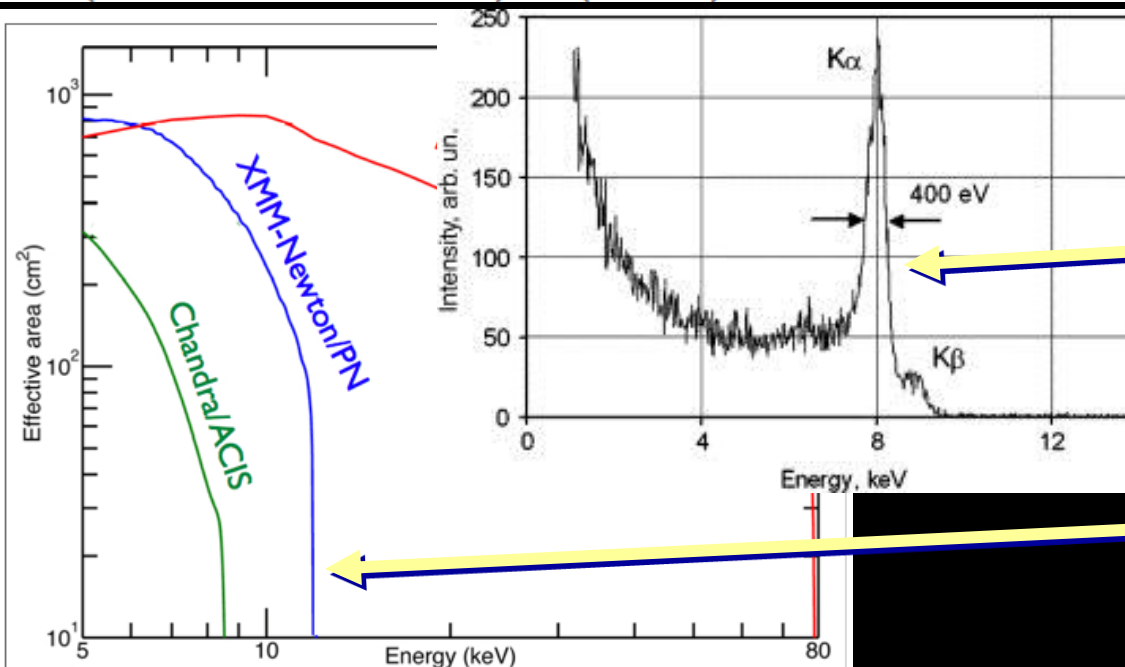
**Detection of ν_s
Decays at $E_{\gamma,s}$
depends on**

➤ $\Phi_{x,s}$

➤ **Spectral Energy
Resolution**
 $\Delta E \simeq E/15$

➤ **ACIS-I Effective
Area**

$A_{\text{eff}}(E_{\gamma,s})$



Detection/Exclusion Criterion:

$$\frac{dN_{\gamma,s}}{dE_{\gamma,s}dt}(\Omega_s) \geq \Delta\mathcal{F}$$

➤ Sterile Neutrino
Decay Signal

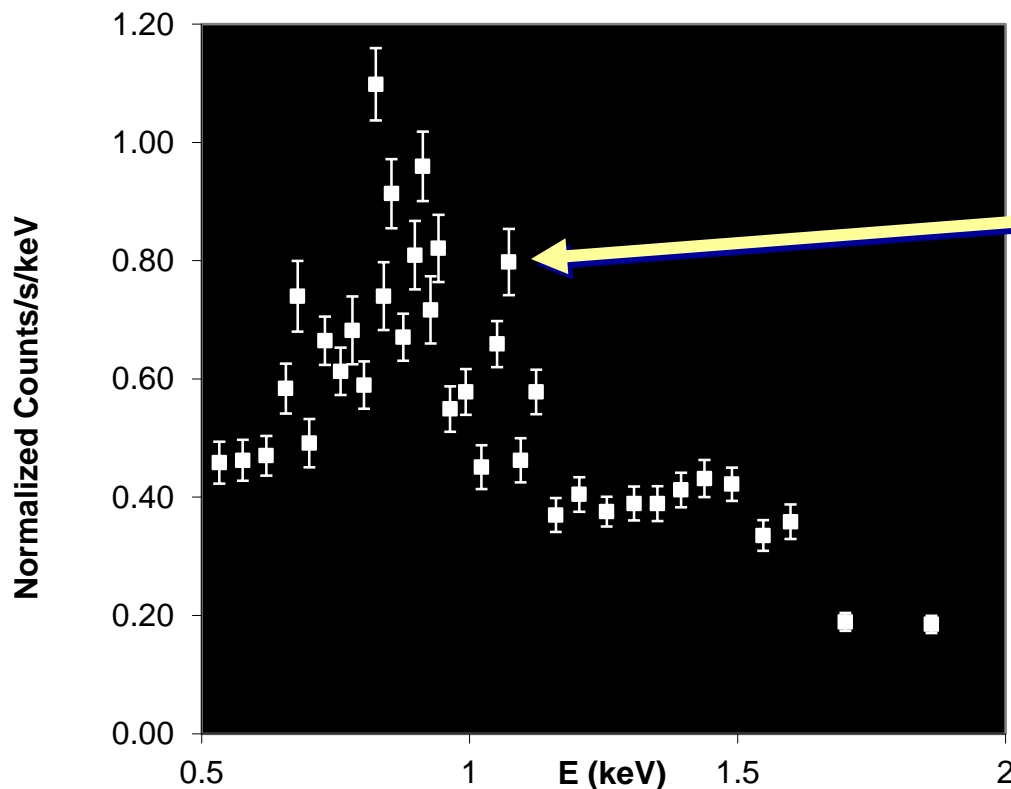
$$dN_{\gamma,s}/dE_{\gamma,s}dt$$

➤ \geq *Chandra Data*

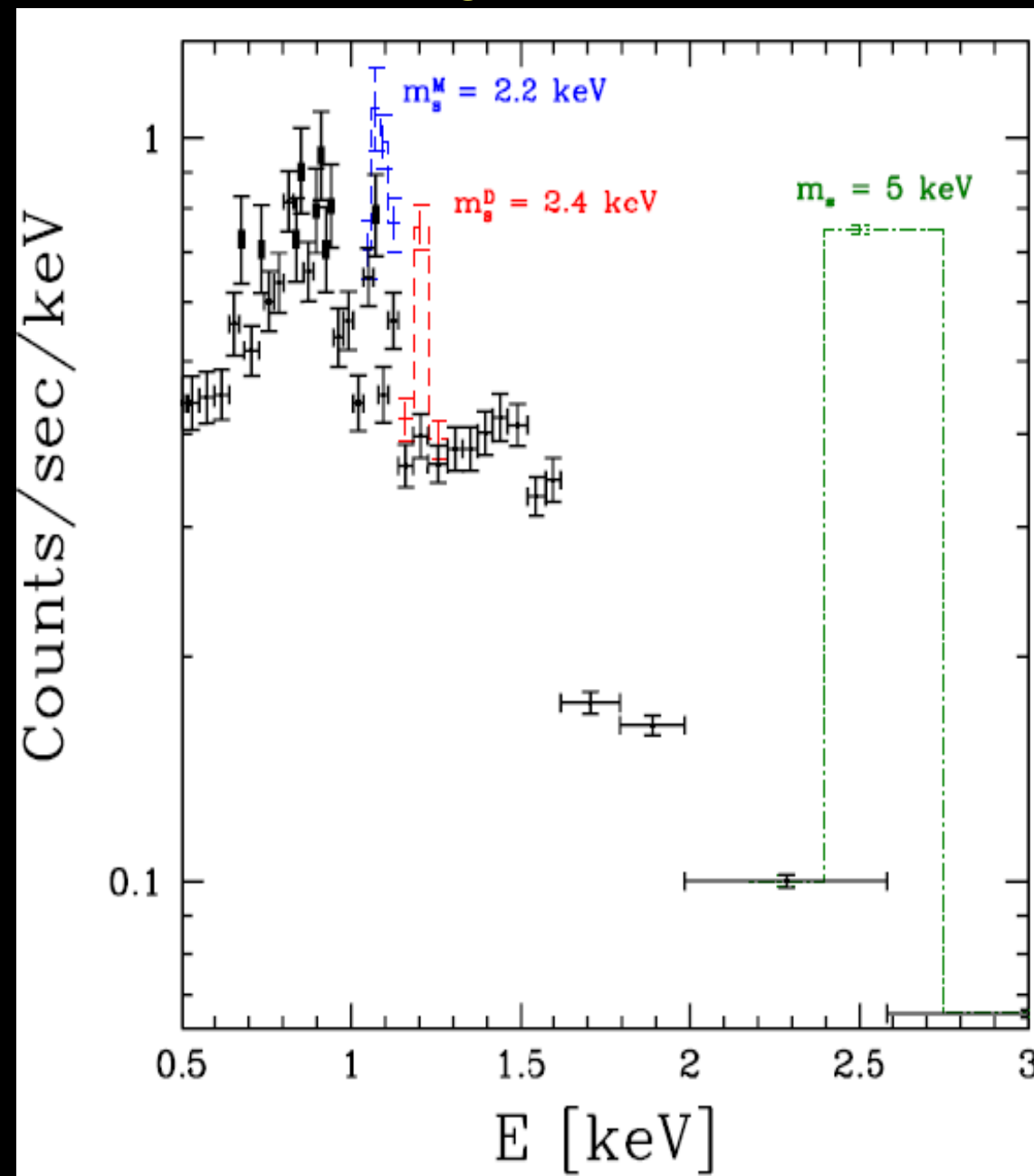
$$\Delta\mathcal{F}$$

➤ in a given bin of
energy

$$E_{\gamma,s}$$



Limits on m_s from *Chandra* Observations of M31



Chandra unresolved X-ray spectrum emitted from 12' - 28' annular region of Andromeda (M31).

Majorana:

$m_s < 2.2$ keV

Dirac:

$m_s < 2.4$ keV

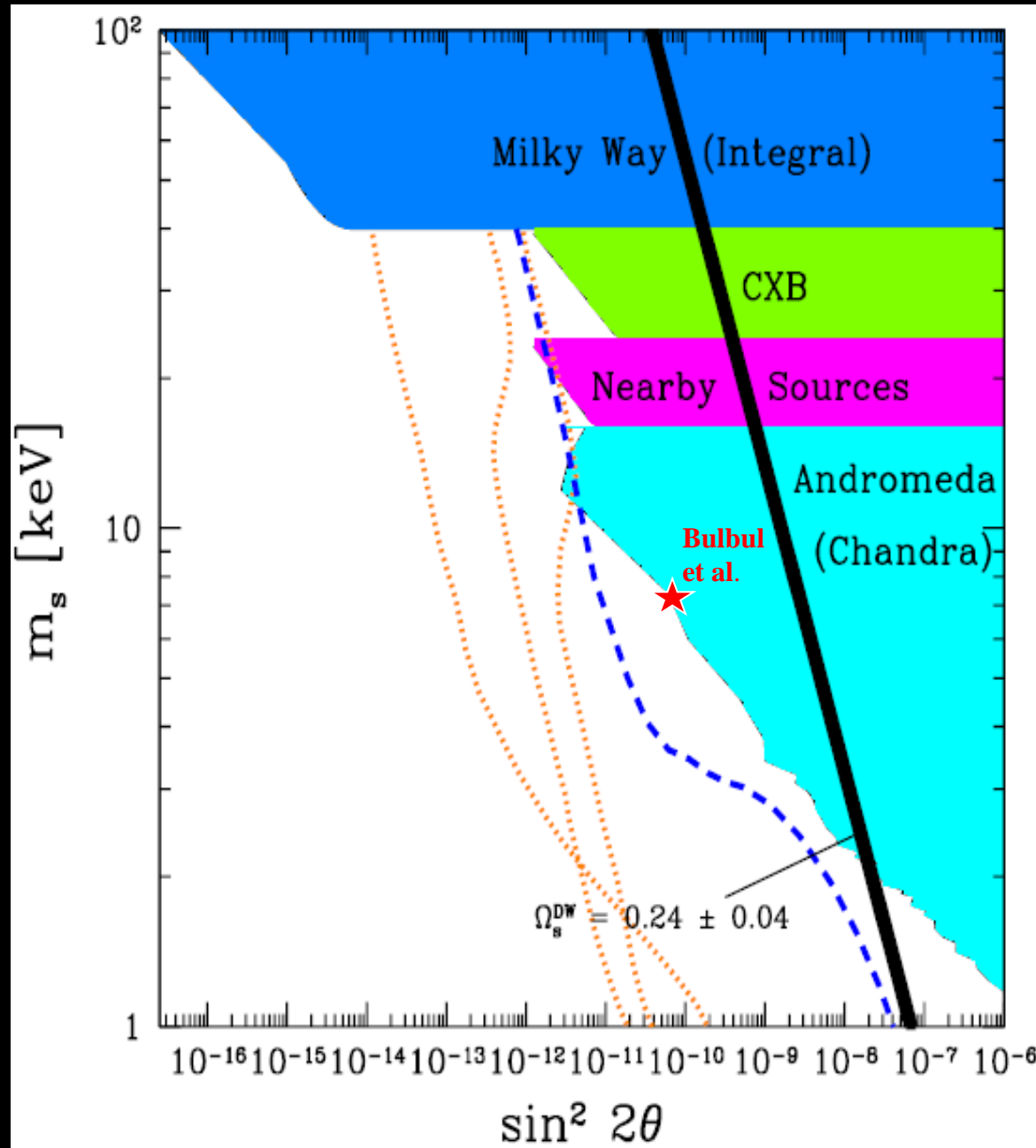
Claimed Detection:

$m_s = 5$ keV

(Loewenstein & Kusenko 2010 [82])

STRONGLY excluded by our data!

Generalized constraints in the $m_s - \sin^2 2\theta$ plane



Exclusion Regions:

Milky Way (Integral):

[77, 78]

Cosmic X-ray Background:

[61, 62]

Andromeda (XMM):

[66]

Andromeda (CXO):

(Watson, Li, & Polley 2012)

Density-Production

Models:

Dodelson-Widrow Model

[3]

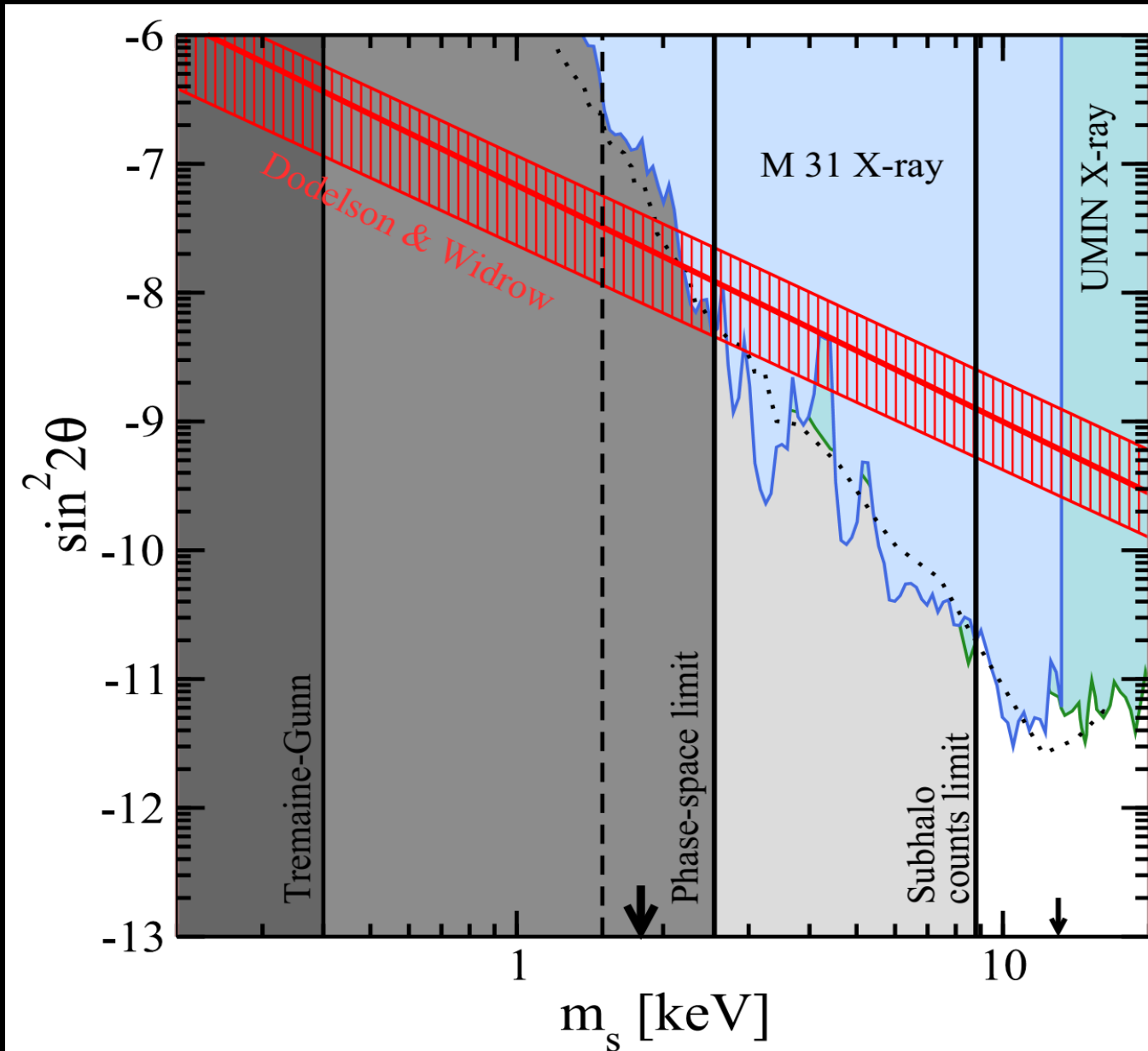
Shi-Fuller Model

[4, 53]

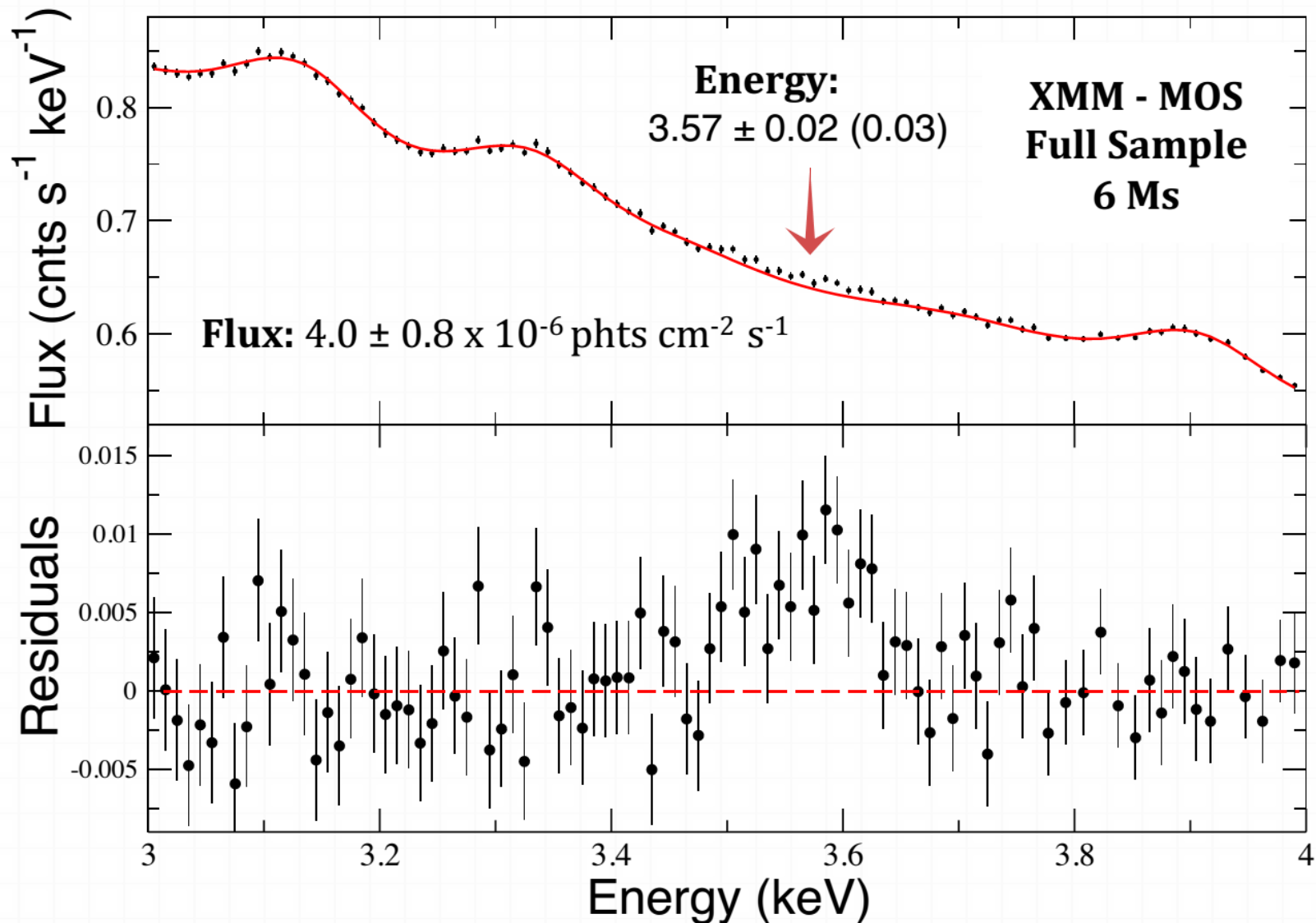
3 L >> 10⁻¹⁰ Lines

[13]

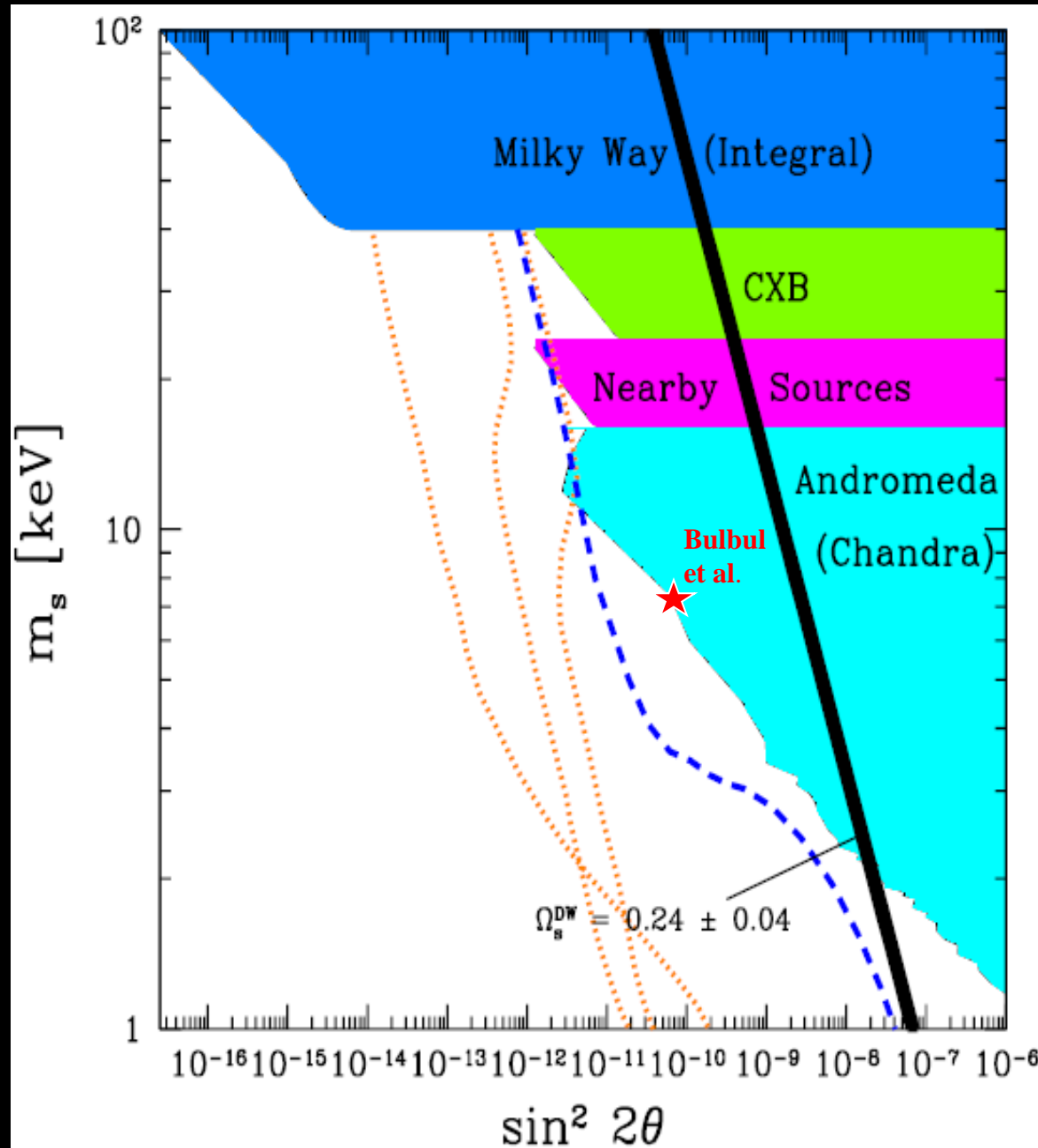
Dodelson-Widrow **Excluded** according to Horiuchi et al. (2014)



Bulbul et al. (2014): Detection of An Unidentified Emission Line



Possible Detection?



Bulbul et al. (2014):

$$m_s = 7.14 \pm 0.1 \text{ keV}$$

$$\sin^2 2\theta = 6.7 \pm 2.5 \times 10^{-11}$$

- ★ Not a background feature
- ★ Not an instrumental line
- ★ Not a detector feature
- ★ Not a modeling artifact
- ★ Comes from all clusters rather than a few dominant bright clusters
- ★ Flux is centrally concentrated

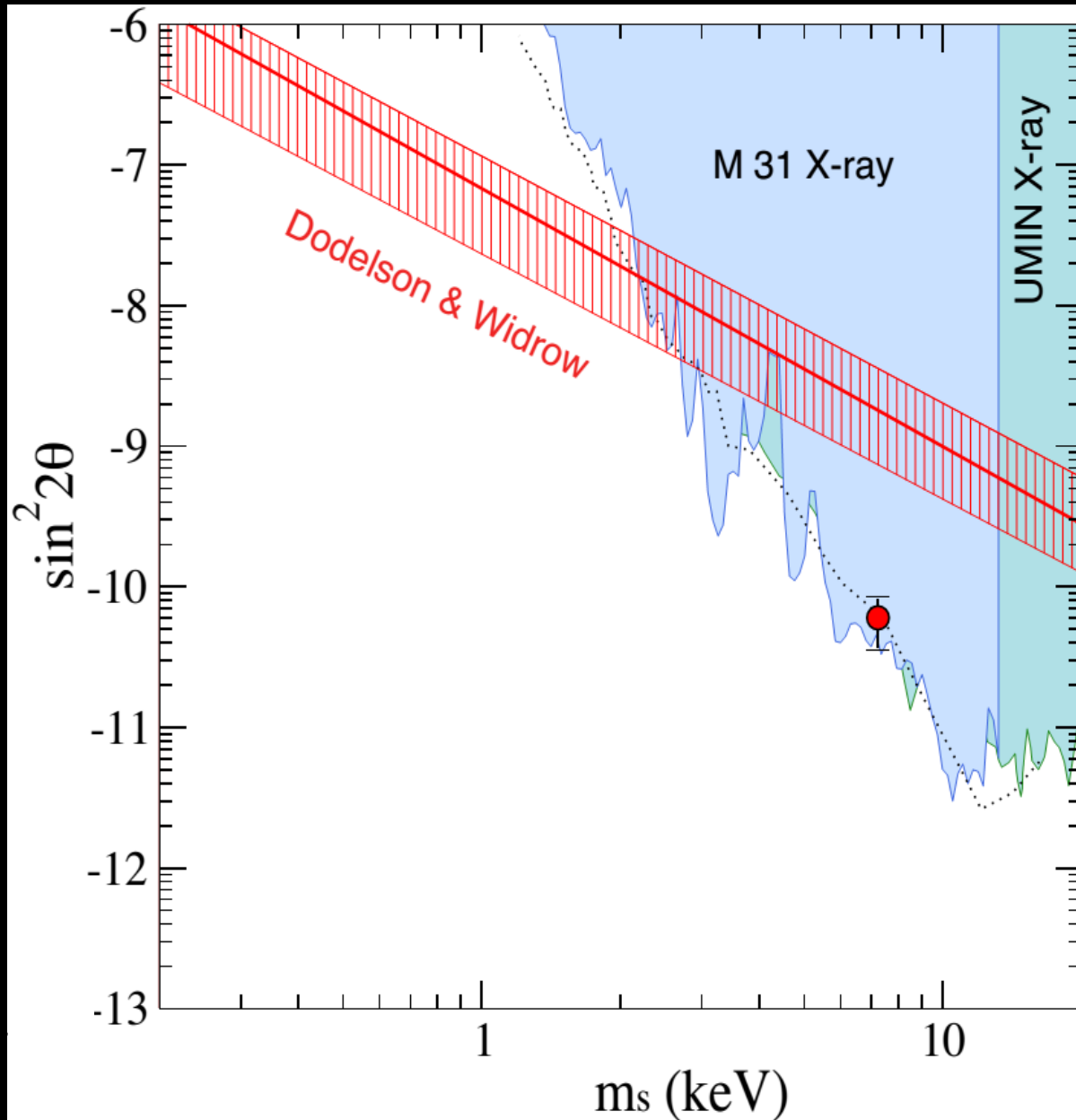
On the cusp of exclusion:

Andromeda (CXO)

(Watson, Li, & Polley 2012)

(Horiuchi et al. 2014)

Bulbul et al. result avoids exclusion at lowest mixing



Bulbul et al. OK if:

$$\sin^2 2\theta \simeq 3-4 \times 10^{-11}$$

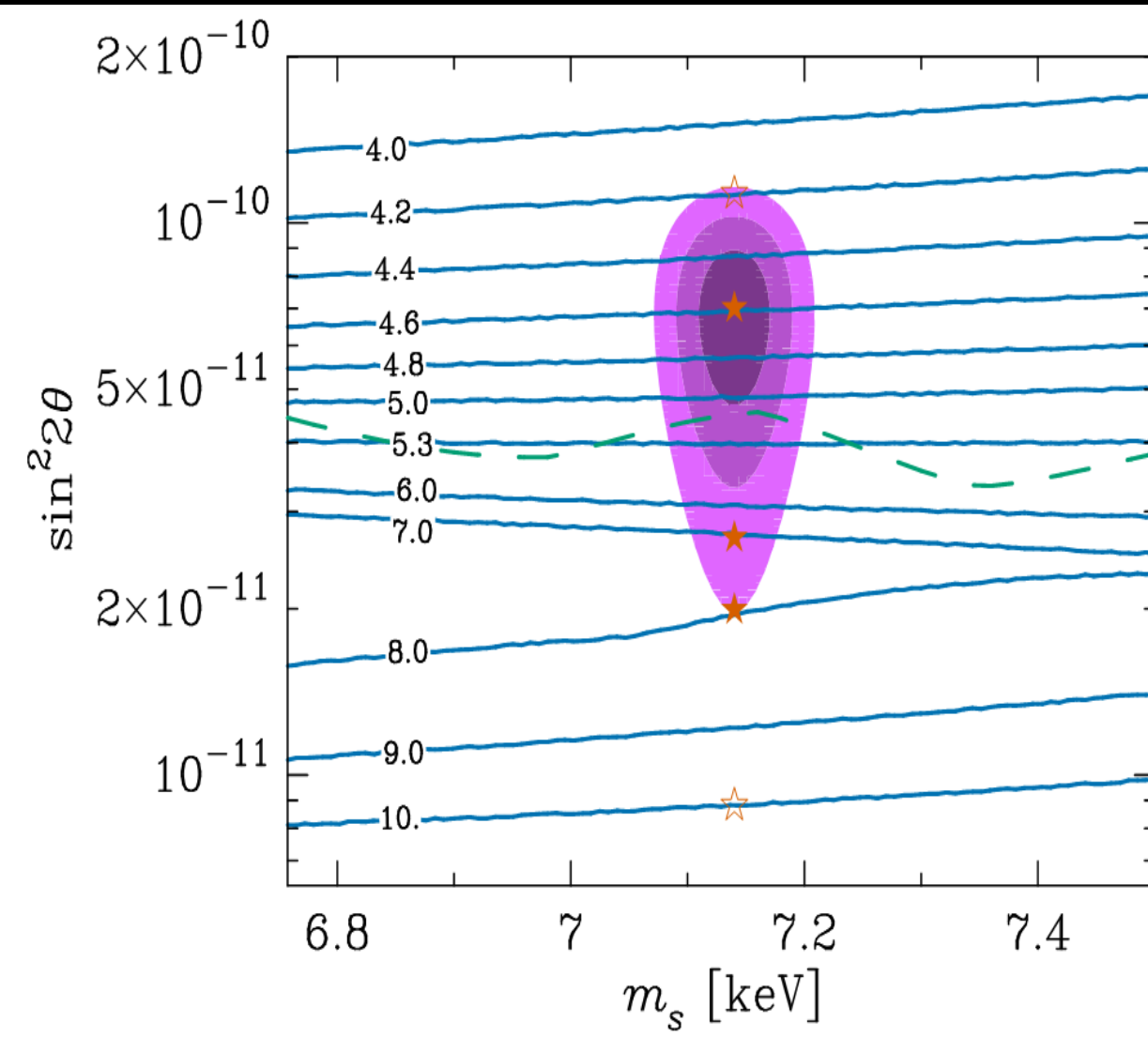
Andromeda (CXO)

Exclusion Constraints:

Dotted (Watson, Li, & Polley 2012)

Solid (Horiuchi et al. 2014)

Shi-Fuller Models (Abazajian 2014)



Bulbul et al.:

$$m_s = 7.14 \pm 0.1 \text{ keV}$$

$$\sin^2 2\theta \simeq 6.7 \times 10^{-11}$$

corresponds to

$$L = 4.6 \times 10^{-4},$$

$$\text{i.e., } L_4 = 4.6$$

IMPORTANT

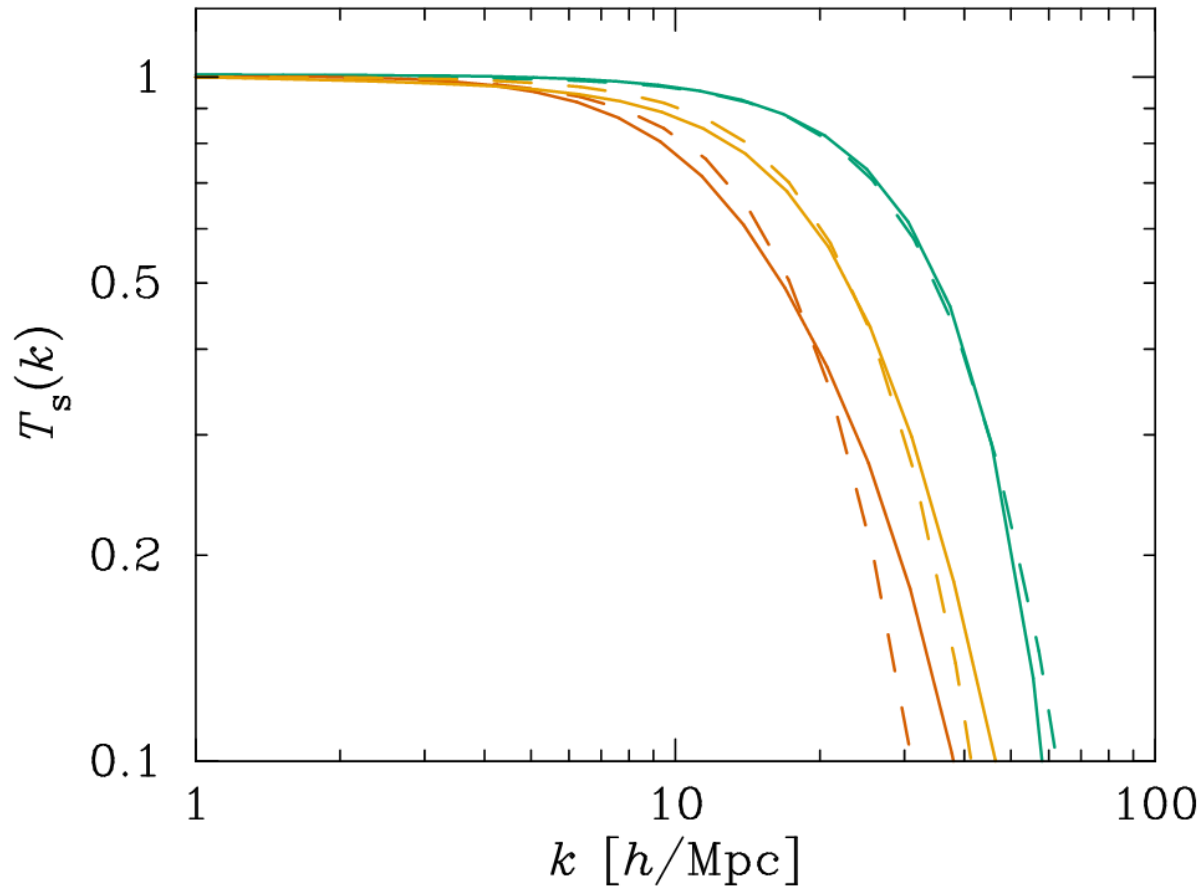
Lower mixing:

$$\sin^2 2\theta \simeq 3 \times 10^{-11}$$

corresponds to

$$L_4 = 7.0$$

WDM Transfer Functions: Shi-Fuller vs. Thermal (Abazajian 2014)



Solid

$L_4 = 8, 7, 4.6$

Dashed

$m_{\text{th}}/\text{keV} = 1.6, 2.0, 2.9$

Galaxy Constraints Satisfied by 2 keV

Thermal Sterile Neutrino (Abazajian 2014)

- **Local Group Phase Space Density and Subhalo Counts:**
 $m_{\text{th}} > 1.7 \text{ keV}$ (Horiuchi et al. 2014)
- **High Redshift Galaxy Counts:**
 $m_{\text{th}} > 1.3 \text{ keV}$ (Schultz et al. 2014)
- **Abundance, Radial Distribution, and Inner Density Profile Crises of Milky Way Satellites solved if:**
 $m_{\text{th}} \simeq 2 \text{ keV}$ (e.g., Lovell et al. 2012 and Abazajian 2014 for additional references)
- **Recall that a 7.14 keV Shi-Fuller ν_s with $L_4 = 7$:
BEHAVES LIKE $m_{\text{th}} \simeq 2 \text{ keV}$!**

Summary I

**DW excluded via phase space constraints
from MW dwarfs.**

(Horiuchi, et al. 2014)

**$m_s = 7.14 \pm 0.1$ keV detection still viable
but close to X-ray exclusion.**

(Bulbul, et al. 2014)

A 7.14 keV Shi-Fuller sterile neutrino with $L_4 = 7$:

- Accounts for X-ray line anomaly found by Bulbul et al.
- Satisfies all galaxy constraints like $m_{\text{th}} \simeq 2$ keV
- Avoids exclusion by Andromeda X-ray Constraints

(Abazajian, et al. 2014)

Phase Space Density Overview I

$$Q \propto \frac{\rho}{\sigma^3}$$

- **For a fermionic thermal relic, Hogan & Dalcanton (2001) find:**

$$Q_{\text{HD}} = \frac{\rho}{(3\sigma^2)^{3/2}} = A Q_* \left(\frac{m}{\text{keV}} \right)^4$$

- **where $A = 5 \times 10^{-4}$ and $Q_* = \frac{M_{\odot}/pc^3}{(\text{km s}^{-1})^3}$**
- **adiabatic invariant**
- **strongly mass-dependent**

Phase Space Density Overview II

- Hogan & Dalcanton's assume a 1-D velocity dispersion.
- As in Horiuchi et al. (2014), we assume MB:

$$Q = \frac{\rho}{(2\pi\sigma^2)^{3/2}} \simeq 0.33Q_{\text{HD}}$$

$$Q_P = A Q_* \left(\frac{m}{\text{keV}} \right)^4$$

- where $A = 1.65 \times 10^{-4}$ and $Q_* = \frac{M_{\odot}/pc^3}{(\text{km s}^{-1})^3}$

Connecting the Past to the Present

- **Galaxy formation processes alter Q by an unknown factor Z :**

$$Z = \frac{Q_P}{Q_0}$$

- **De Vega & Sanchez (2010) explored a number of analytical methods to find Z , concluding that**
 - **$1 \leq Z \leq 10^4$, in agreement with simulations**
 - **the mass of a thermal relic DM particle is $\sim \text{keV}$:**

$$\frac{m_{\text{th}}}{\text{keV}} = \left(\frac{Q_p}{A} \right)^{1/4} = \left(\frac{Z Q_0}{A} \right)^{1/4} \simeq 1 - 10$$

Goals of Our Project

1. Determine Z directly from the dwarf galaxy data to produce a model-independent mapping between Q_p and Q_0 .
2. Use this empirical Z factor to determine the DM particle mass – both for thermal and non-thermal relics.
3. Identify primordial dwarf galaxies – i.e., systems for which $Q_0 \simeq Q_p$.
4. Draw insights from these primordial objects about the formation and evolution of galaxies.

Dwarf Galaxy Data (Sample)

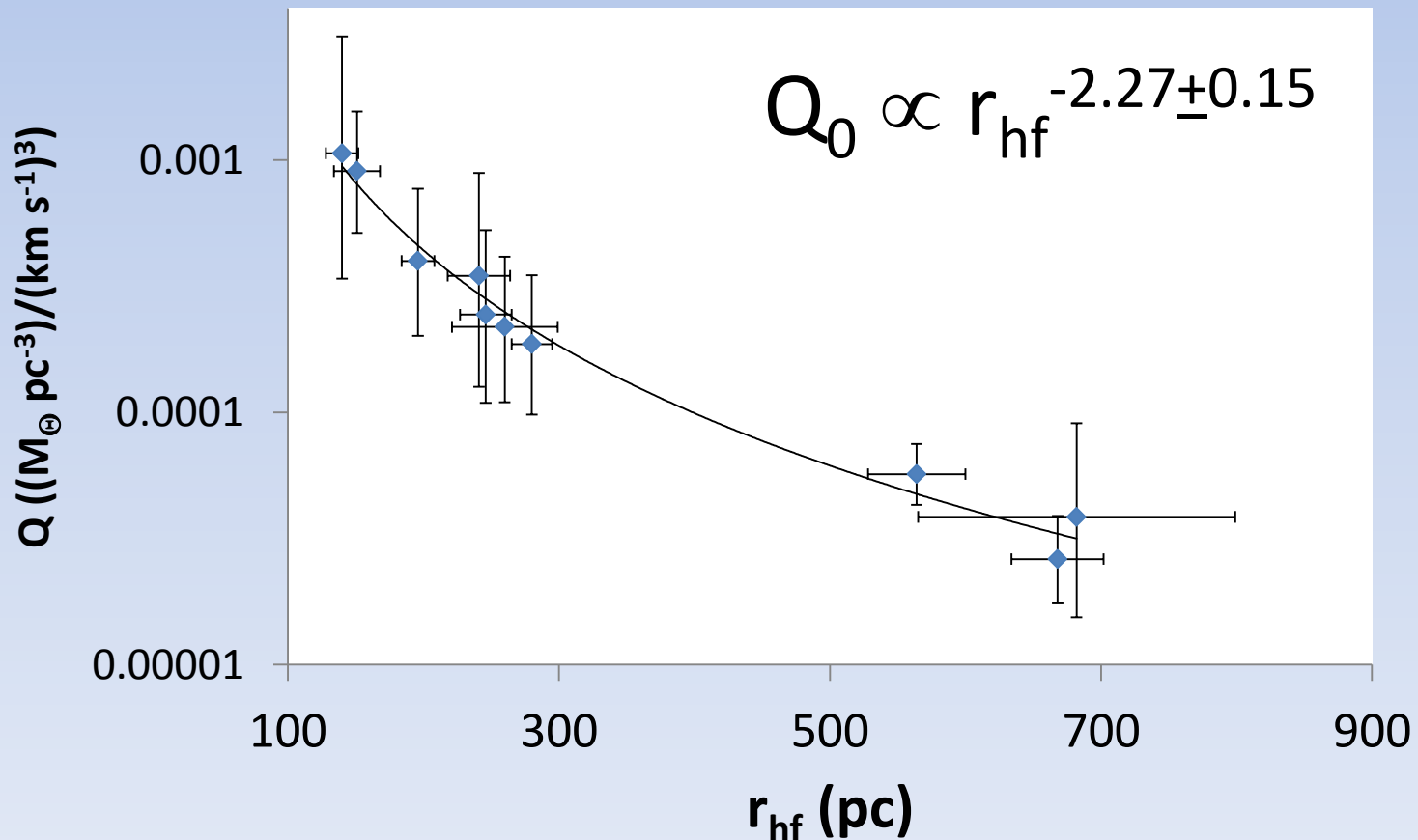
- Data for 23 dSphs from Walker et. al. (2009)

Dwarf	σ (km/s)			ρ ($M_{\odot} \text{ pc}^{-3}$)			r_{hf} (pc)			$M(r_{\text{hf}})$ ($10^7 M_{\odot}$)		
Carina	6.6	\pm	1.2	0.1	\pm	0.04	241	\pm	23	0.61	\pm	0.23
Draco	9.1	\pm	1.2	0.3	\pm	0.08	196	\pm	12	0.94	\pm	0.25
Fornax	11.7	\pm	0.9	0.042	\pm	0.007	668	\pm	34	5.3	\pm	0.9
Leo I	9.2	\pm	1.4	0.19	\pm	0.06	246	\pm	19	1.2	\pm	0.4
Leo II	6.6	\pm	0.7	0.26	\pm	0.06	151	\pm	17	0.38	\pm	0.09
Sculptor	9.2	\pm	1.1	0.17	\pm	0.05	260	\pm	39	1.3	\pm	0.4
Sextans	7.9	\pm	1.3	0.019	\pm	0.007	682	\pm	117	2.5	\pm	0.9
U Minor	9.5	\pm	1.2	0.16	\pm	0.04	280	\pm	15	1.5	\pm	0.4
C Ven I	7.6	\pm	0.4	0.025	\pm	0.003	564	\pm	36	1.9	\pm	0.2
U Ma II	6.7	\pm	1.4	0.32	\pm	0.14	140	\pm	25	0.36	\pm	0.16

Q – r_{hf} Power-Law Relation

- The power-law relations from Walker et al. (2009):

$$\rho \propto r_{\text{hf}}^{-1.6}; \sigma \propto r_{\text{hf}}^{0.2} \rightarrow Q \propto \frac{\rho}{\sigma^3} \propto r_{\text{hf}}^{-2.2}.$$



Phase Space Density of the DM

- Q_0 shown in the previous plot is based on *stellar* velocity dispersions, σ_* .

- Horiuchi et al. (2014) find

$$\eta_* = \sigma / \sigma_* = 1.5 \pm 0.2$$

- Adopting this correction factor, we find

$$Q_{0,\text{DM}} = (1.61 \pm 0.42) Q_* \left(\frac{r_{hf}}{\text{pc}} \right)^{-n}$$

- where $n = 2.27 \pm 0.15$ and $Q_* = \frac{M_\odot / \text{pc}^3}{(\text{km s}^{-1})^3}$

Using $Q(r_{\text{hf}})$ to find Z

- We can rewrite the $Q(r_{\text{hf}})$ power-law in terms of:
 - the unknown, primordial Q_p
 - and
 - an unknown radial scale, r_p :

$$Q_0 = Q_P \left(\frac{r_p}{r_{\text{hf}}} \right)^n = Q_P / Z_{\text{em}}$$

$$Z_{\text{em}} = (r_{\text{hf}} / r_p)^n$$

- Thus, determining r_p is the key to the empirical Z factor.

Empirical Limits on r_p

Q can only decrease (Liouville's Theorem), so

$$Z = (r_{hf}/r_p)^n \geq 1$$

$$r_p \leq r_{hf,min}$$

Minimum r_{hf} values:

- Willman 1: $r_{hf} = 25 \pm 6$ pc
- Segue 1: $r_{hf} = 29 \pm 7$ pc
- Segue 2: $r_{hf} = 34 \pm 5$ pc
- Leo V: $r_{hf} = 42 \pm 5$ pc

$$r_p \lesssim 19 - 47 \text{ pc.}$$

Finding r_p analytically

- **Determine when the virial mass (Boylan-Kolchin et al. 2013) of the MW halo entered the horizon:**
 - **Earliest time causal processes could affect the PSD of DM in a MW-sized overdensity and in its primordial subhalo overdensities**

$$M_{\text{MW}} = \frac{4}{3}\pi\rho_{m,0}(1+z)^3 \left(\frac{d_H(z)}{2}\right)^3 = 1.6^{+0.8}_{-0.6} \times 10^{12} M_{\odot}$$

- **This occurs when**

- $z_{\text{MW}} = 9.4^{+1.2}_{-1.6} \times 10^4$

- $r_p = d_H(z_{\text{MW}})/2 = 26.7^{+8.3}_{-7.2} \text{ pc}$

which agrees with empirical limits.

Q_p Values + DM Particle Mass

- Max/Min Q_0 ratio is $\sim 10^4$

$$Q_p = Z_{\text{em}} Q_0$$

- Max/Min Q_p differ by ~ 4.5

$$\frac{m_{\text{th}}}{\text{keV}} = \left(\frac{Z_{\text{em}} Q_0}{A} \right)^{1/4} = \left(\frac{\left(\frac{r_{hf}}{r_p} \right)^n Q_0}{A} \right)^{1/4}$$

- Max/Min m_{th} values differ by ~ 1.5

Including all galaxy data uncertainties

- $1 < Z < 10^4$
- $0.74 < m_{\text{th}}/\text{keV} < 2.8$ (mean 1.55 keV)

Non-thermal DM

- If the DM particle is a sterile neutrino, we can use the following transformation equations (e.g., Viel et al. 2005; Abazajian 2014) to find the corresponding non-thermal limits:

$$m_{s,DW} = 4.27\text{keV} \left(\frac{m_{th}}{\text{keV}} \right)^{4/3} \left(\frac{\Omega_{m,0} h^2}{0.1371} \right)^{-1/3} \simeq 1.5 m_{s,SF}$$

- Applying these transformations, we find:

2.9 < m/keV < **16.9** (Dodelson-Widrow) **X** (Watson et al. 2012)

1.9 < m/keV < **11.2** (Shi-Fuller) **Bulbul et al. (2014) OK**

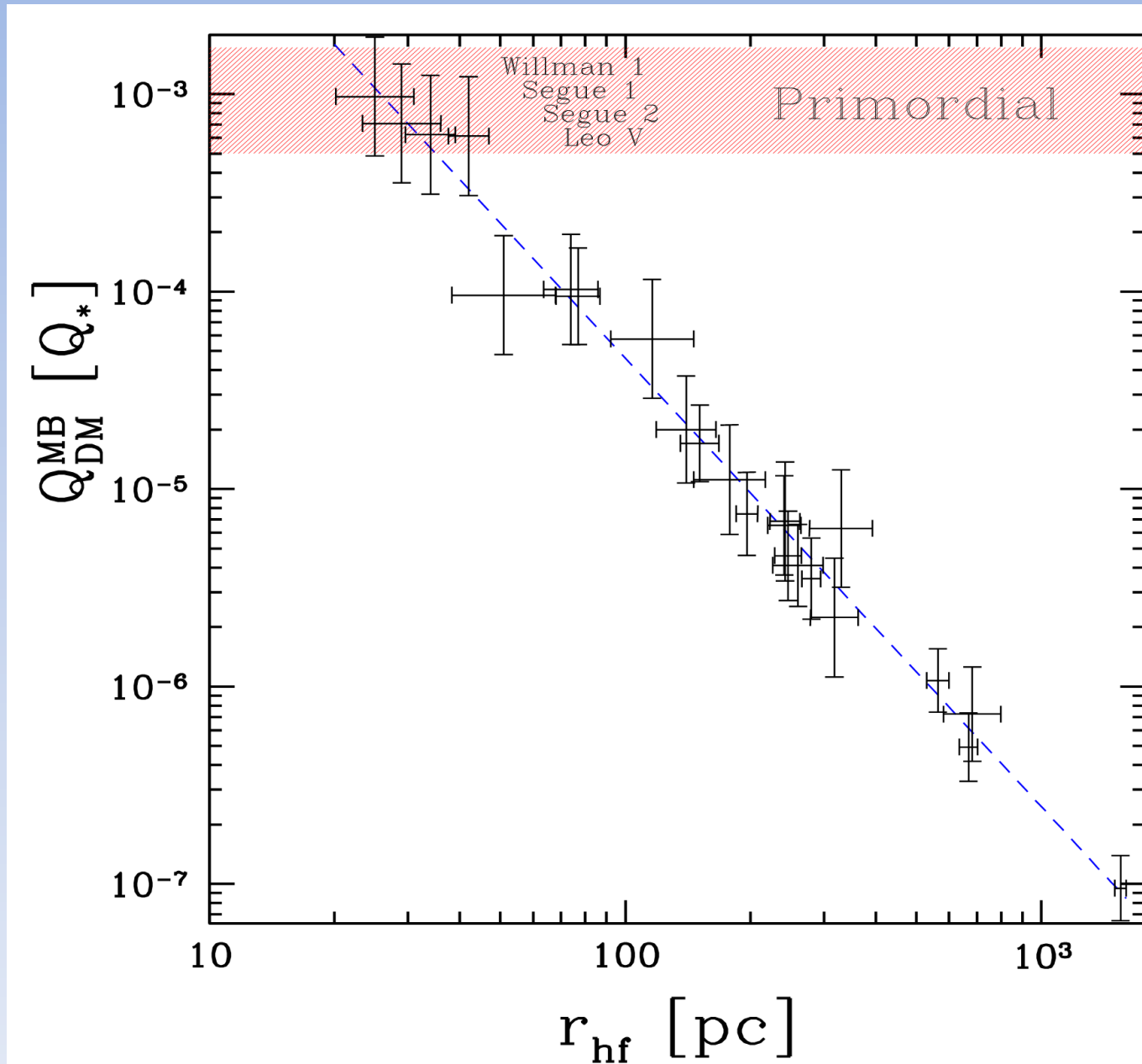
- Alternative transformations (deVega & Sanchez 2013):

$$m_v^{DW} = 2.85\text{keV} \left(\frac{m_{th}}{\text{keV}} \right)^{4/3} ; m_v^{SF} \cong 2.55 m_{th}$$

1.9 < m/keV < **11.3** (Dodelson-Widrow) **X** (Horiuchi et al. 2014)

1.9 < m/keV < **7.2** (Shi-Fuller) **Bulbul et al. (2014) OK**

Identification of Primordial Objects



Implications for Galaxy Formation/Evolution

- If the 4 “primordial” dSphs have evolved undisturbed, their current densities should match virial values:

$$\rho_{\text{obs}} = 358\rho_{\text{b,vir}} = 358\rho_{M,0}(1 + z_{\text{coll}})^3$$

- Using $\rho_{\text{obs}} = \rho(r_{\text{hf}})$,
- $34 < z_{\text{coll}} < 78$ (25 Myrs – 85 Myrs)
- Nice agreement with early formation epoch of first stars in sterile neutrino cosmological models, e.g., Biermann and Kusenko (2006).

The Universal dSph DM Halo and the Free-Streaming Scale

- Observed properties of MW dSphs suggest that they formed from a consistent DM Halo (Wolf et al. 2013):

$$M_{\text{MW Sat}}^{\text{Univ}} = (3.0 \pm 0.5) \times 10^9 M_{\odot}$$

- Does this universality suggest a special scale, perhaps the free-streaming mass scale?

$$M_{fs} = 4/3\pi\rho_{0,m} \left(\frac{\lambda_{fs}}{2}\right)^3 = 6.4 \times 10^{10} M_{\odot} \left(\frac{m_{\text{th}}}{\text{keV}}\right)^{-4}$$

- Taking $M_{\text{MW Sat}}^{\text{Univ}} = M_{fs}$ yields

$$m_{\text{th}} = 2.15 \pm 0.1 \text{ keV}$$

Summary II

- Using data from Walker et. al. (2009), we found a strong correlation between Q and r_{hf} for Milky Way dwarf satellite galaxies.
- Determining the primordial radial scale r_p , we established Q_p and limits on the DM particle mass:
 - $0.74 < m_{\text{th}}/\text{keV} < 2.8$ (mean 1.55 keV)
 - **DW ruled out, Shi-Fuller $1.9 < m_{\text{SF}}/\text{keV} < 11.2$**
- Comparing to Q_p , we see 4 primordial MW dSphs: Leo V, Segue 1, Segue 2, and Willman 1.
- Implied Virialization Epochs for primordial dSphs
 $34 < z_{\text{coll}} < 78$ (25 Myrs – 85 Myrs)
- Interpreting Univ. dSph DM Halo as M_{fs} implies
 $m_{\text{th}} = 2.15 \pm 0.1 \text{ keV}$

Conclusions

DW excluded via M31 X-ray constraints and phase space density constraints from MW dSphs.

(Watson et al. 2012, Horiuchi, et al. 2014, This Work)

A 7.14 keV Shi-Fuller sterile neutrino with $L_4 = 7$:

- Accounts for X-ray line anomaly found by Bulbul et al.
- Satisfies all galaxy constraints like $m_{\text{th}} \simeq 2 \text{ keV}$
- Avoids exclusion by Andromeda X-ray Constraints

(Abazajian, et al. 2014)

- Consistent with Phase Space Density Constraints on MW dSphs
- Consistent with Free-Streaming Mass Scale implied by MW dSphs

(Horiuchi et al. 2014 + This Work)